



# HEAT CONDUCTION

Heat conduction modelling .....	1
Case studies.....	2
Analytical solutions.....	3
Conduction shape factor (steady state) .....	3
Reduction to the main dimension (steady state) .....	5
Planar, cylindrical, and spherical energy sources, internal or interfacial .....	6
Multilayer composite walls.....	7
Critical radius.....	8
Rods and fins.....	8
Heat source moving at steady state along a rod.....	11
Reduction by dimension similarity (unsteady state).....	12
Energy deposition in unbounded media.....	13
Thermal contact in semi-infinite media .....	17
Freezing and thawing .....	19
Reduction by separation of variables .....	20
Unsteady problems in 1-D .....	21
Periodic solutions in 1-D.....	26
Steady problems in 2-D.....	27
Other analytical methods to solve partial differential equations.....	31
Duhamel`s theorem.....	32
Numerical solutions .....	32
Global fitting .....	34
Lumped network .....	37
Spectral methods.....	38
Residual fitting.....	38
Collocation method.....	39
Least square method (LSM).....	39
Galerkin method.....	39
Finite differences.....	40
Finite elements .....	44
Boundary elements.....	45

## HEAT CONDUCTION MODELLING

Heat transfer by conduction (also known as diffusion heat transfer) is the flow of thermal energy within solids and non-flowing fluids, driven by thermal non-equilibrium (i.e. the effect of a non-uniform temperature field), commonly measured as a heat flux (vector), i.e. the heat flow per unit time (and usually unit normal area) at a control surface.

[The basics of Heat Transfer \(what is it, what for, its nomenclature, case studies, and the general view on how heat-transfer problems are solved and analysed\), is to be found aside, and assumed already covered.](#)

As explained there, the solution to heat-transfer problems can be directly applied, with the appropriate change of variables, to mass-transfer problems.

The general equations for heat conduction are the energy balance for a control mass,  $dE/dt = \dot{Q} + \dot{W}$ , and the constitutive equations for heat conduction (Fourier's law) which relates heat flux to temperature gradient,  $\vec{q} = -k\nabla T$ . Their combination:

$$\left. \begin{aligned} \dot{Q} = \frac{dH}{dt} \Big|_p &= KA\Delta T = -\int_A \vec{q} \cdot \vec{n} dA \\ \vec{q} &= -k\nabla T \end{aligned} \right\} \Rightarrow \dot{Q} = \frac{dH}{dt} \Big|_p = \int_A k\nabla T \cdot \vec{n} dA = \int_V \nabla \cdot (k\nabla T) dA \rightarrow \quad (1)$$

when applied to an infinitesimal volume, yield the partial differential equation (PDE) known as heat equation, or diffusion equation, as [explained aside](#):

$$\rho c \frac{\partial T}{\partial t} = k\nabla^2 T + \phi - \rho c \vec{v} \cdot \nabla T \quad (2)$$

where the last two terms in (2) come from separating enthalpy changes in a temperature-dependent term ( $dH=V\rho c dT$ ), and the rest  $dH=-V\phi dt$  (to account for a possible energy dissipation term,  $\phi$  [ $W/m^3$ ]), and a possible choice of coordinate system moving relative to the material at velocity  $\vec{v}$  (i.e., by splitting the convective derivative  $dH/dt = \partial H/\partial t + \vec{v} \cdot \nabla H$ ). Many times, thermal conductivity in (2) is to be found under the thermal diffusivity variable:  $a \equiv k/(\rho c)$ .

In this presentation we embark into generic analytical and numerical methods to solve the heat conduction equations (2) within the bounding conditions of each particular problem (i.e., a PDE with some initial and boundary conditions, BC). It is worth to mention now that, in the theory of Heat Transfer, initial and boundary conditions are always neatly drawn, and great effort is devoted to solving the heat equation, whereas, in real Heat Transfer practice, initial and boundary conditions are so loosely defined that well-founded heat-transfer knowledge is needed to model them, and solving the equations is just a computer chore.

## Case studies

To better illustrate the different methods of solving heat-conduction problems, we are considering the two following paradigms:

- **Rod-heated-at-one-end.** This is the heating-up of a metal rod in ambient air by an energy source at one end, as when holding a wire with our fingers from one end. To be more precise, we may think of an aluminium rod of length  $L=0.1$  m and diameter  $D=0.01$  m, being heated at one end with  $\dot{Q}_0=10$  W (from an inserted small electrical heater), while being exposed to a ambient air at  $T_\infty=15$  °C with an estimated convective coefficient  $h=20$  W/(m<sup>2</sup>·K), and take for aluminium  $k=200$  W/(m·K),  $\rho=2700$  kg/m<sup>3</sup> and  $c=900$  J/(kg·K). The name rod usually refers to centimetric-size elements; for much smaller rods, the word wire (or spine), is more common, and the word beam for much larger elements. This example is a quasi-one-dimensional unsteady heat-transfer problem, which has a non-trivial steady state temperature profile and demonstrates the tricky approximations used in modelling real problems (e.g. grasping a long thermometer at the sensitive end).

- **Cylinder-cooling-in-a-bath.** This is the cooling-down of a hot cylinder in a water bath. To be more precise, we may think of a food can of length  $L=0.1$  m and  $D=0.05$  m in diameter, taken out of a bath at  $T_1=100$  °C (e.g. boiling water) and submerged in a bath of ambient water at  $T_\infty=15$  °C with an estimated convective coefficient of  $h=500$  W/(m<sup>2</sup>·K), taking for the food  $k=1$  W/(m·K),  $\rho=1000$  kg/m<sup>3</sup> and  $c=4000$  J/(kg·K), and neglecting the effect of the thin metal cover. This is a three-dimensional unsteady problem of practical relevance in materials processing.

## ANALYTICAL SOLUTIONS

Analytical solutions are, in principle, the best outcome for a problem, not because they are more accurate than numerical solutions (exactness is outside the physical realm), but because they are stricter, in the sense that the influence of the parameters is explicitly shown in the answer (i.e. they have far more information content).

Analytical solutions to heat transfer problems reduce to solving the PDE (2), i.e. the heat equation, within a homogeneous solid, under appropriate initial and boundary conditions (IC and BC, which may include convective and radiative interactions with the environment). Many analytical solutions refer just to the simple one-dimensional planar problem obtained from (2) when dropping the dissipation and the convective terms, i.e. to the classical parabolic PDE:

$$\frac{\partial^2 T}{\partial x^2} - \frac{1}{a} \frac{\partial T}{\partial t} = 0 \quad (3)$$

and practically all analytical solutions refer to the much richer two-dimensional equation with heat sources and a possible relative coordinate-motion:

$$\frac{1}{r^n} \frac{\partial}{\partial r} \left( r^n \frac{\partial T}{\partial r} \right) + \frac{\partial^2 T}{\partial z^2} - \frac{\rho c v}{k} \frac{\partial T}{\partial z} + \frac{\phi(r, z, t)}{k} - \frac{1}{a} \frac{\partial T}{\partial t} = 0 \quad (4)$$

where  $n=1$  for cylindrical geometries and  $n=2$  for spherical geometries ( $n=0$  for planar geometries like in (3)), and  $v$  is the velocity of the solid material relative to a  $z$ -moving reference frame (e.g. a travelling sample in a furnace, or a moving heater along a sample at rest).

Several different approaches may be used to find analytical solutions to PDEs like (3) and (4): dimension reduction, reduction by similarity, separation of variables, Green's function integrals, Laplace transforms, etc., and, although this might be thought just a mathematical burden, it teaches a lot on thermal modelling, shows with little effort the key effect of boundary conditions, and provides reliable patterns against which practical numerical solutions (full of initial uncertainties) can be checked with confidence.

### Conduction shape factor (steady state)

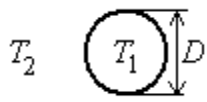
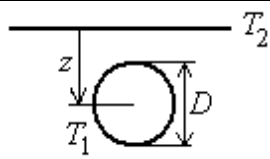
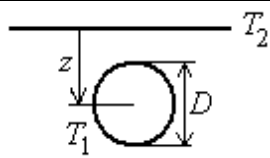
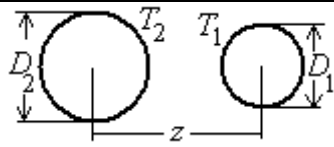
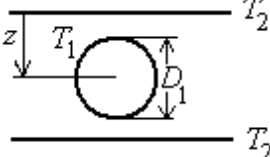
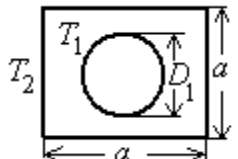
The generic aim in heat conduction problems (both analytical and numerical) is at getting the temperature field,  $T(x,t)$ , and later use it to compute heat flows by derivation. However, for steady heat conduction between two isothermal surfaces in 2D or 3D problems, particularly for unbound domains, the simplest

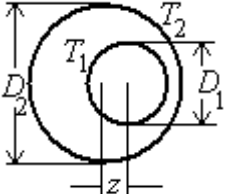
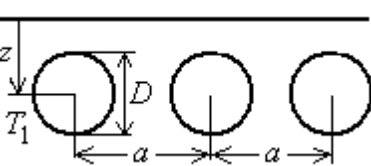
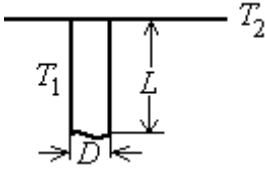
way to present analytical solutions is by means of the so-called conduction shape factor  $S$ , defined by  $\dot{Q} = kS\Delta T$ , that separates geometrical effects ( $S$ ), from material effects ( $k$ ), which appear mixed-up in the general equation  $\dot{Q} = KA\Delta T$ .

For instance, the shape factor between two parallel plates of frontal area  $A$ , separated a distance  $L$  (with  $A \gg L^2$ ), is  $S=A/L$ , meaning that the heat transfer rate through a planar wall of thickness  $L$  is  $\dot{Q} \equiv kS(T_1 - T_2) = k(A/L)(T_1 - T_2)$ , as Fourier's law teaches.

Table 1 gives some such shape factors, what may serve as recipes to solve some canonical heat-conduction problems, but teach nothing on the subject (provide no insight for non-tabulated cases). Notice that symmetry can be applied to extend applications; e.g. we may wonder how hot would become a small electronic device sandwiched between two media, one of thermal conductivity  $k$ , and the other insulating (i.e. with a much lower  $k$ ), when dissipating a power  $\dot{W}$ ; the answer is that, at the steady state, the component will reach a temperature  $T_1$  such that  $\dot{W} = \dot{Q} = kS(T_1 - T_2)$ , with  $S$ -values from (5) for a semi-infinity configuration, i.e.  $S=\pi D$  for a hemispherical component, or  $S=2D$  for a thin disc shape (e.g. if a  $D=1$  cm disc-shape chip dissipates  $\dot{W}=10$  W through a much larger silicon substrate of  $k=150$  W/(m·K) (with the other semi space made of insulating plastic), the chip temperature will rise  $\Delta T = \dot{W}/(kS) = 10/(150 \cdot 0.02) = 3.3$  K.

Table 1. Conduction shape factors,  $S$ , defined by  $\dot{Q} = kS(T_1 - T_2)$  at steady state\*.

Sphere, thin disc, or cube, to unbound medium		$S=2\pi D$ for a sphere $S=4D$ for a thin disc $S=8.24D$ for a cube	(5)
Sphere against unbound planar surface		$S = \frac{2\pi D}{1 - \frac{D}{4z}} \xrightarrow{z \gg D} 2\pi D$	(6)
Long cylinder ( $L \gg D$ ) against unbound parallel planar surface (notice that $S \xrightarrow{z \rightarrow \infty} 0$ )		$S = \frac{2\pi L}{\text{arccosh}\left(\frac{2z}{D}\right)} \xrightarrow{z \gg D} \frac{2\pi L}{\ln\left(\frac{4z}{D}\right)}$	(7)
Two parallel long cylinders		$S = \frac{2\pi L}{\text{arccosh}\left(\frac{4z^2 - D_1^2 - D_2^2}{2D_1D_2}\right)}$	(8)
Long cylinder between planar surfaces		$S = \frac{2\pi L}{\ln\left(\frac{8z}{\pi D}\right)}$	(9)
Long cylinder within a square		$S = \frac{2\pi L}{\ln\left(\frac{1.08a}{D}\right)}$	(10)

Long cylinder within a coaxial cylinder (notice that $S \xrightarrow{z \rightarrow 0} \frac{2\pi L}{\ln(D_2/D_1)}$ )		$S = \frac{2\pi L}{\operatorname{arccosh}\left(\frac{D_1^2 + D_2^2 - 4z^2}{2D_1D_2}\right)}$	(11)
Row of $N$ long cylinders against planar surface		$S = \frac{2\pi LN}{\ln\left(\frac{2a}{\pi D} \sinh\left(\frac{2\pi z}{a}\right)\right)}$	(12)
Long cylinder flush with a planar surface		$S = \frac{2\pi L}{\ln\left(\frac{4L}{D}\right)}$	(13)

**Exercise 1.** Heating of a  $4.6 \text{ m}^2$  room is achieved by 10 equally spaced hot-water pipes of 12 mm external diameter, 6 m long, buried 25 mm underneath the floor (at their axes). Assuming that the heating needed to keep an average of  $21 \text{ }^\circ\text{C}$  in the room is 3 kW, and values of  $k=1 \text{ W}/(\text{m}\cdot\text{K})$  for the floor materials and  $h=10 \text{ W}/(\text{m}^2\cdot\text{K})$  for natural convection in air, find the required hot-water temperature and the temperature in the floor surface.

**Solution.** By making use of the conduction shape factor in Table 1, for a row of long cylinders against planar surface, we have:

$$\dot{Q} = kS(T_2 - T_1) = hA(T_1 - T_0), \quad \text{with } S = \frac{2\pi LN}{\ln\left(\frac{2a}{\pi D} \sinh\left(\frac{2\pi z}{a}\right)\right)} \quad (14)$$

with the unknowns being  $T_2$  (pipe temperature) and  $T_1$  (floor temperature), and the data:  $T_0=21 \text{ }^\circ\text{C}$ ,  $\dot{Q} = 3000 \text{ W}$ ,  $k=1 \text{ W}/(\text{m}\cdot\text{K})$ ,  $L=6 \text{ m}$ ,  $a=W/N=4/10=0.4 \text{ m}$ , and  $h=10 \text{ W}/(\text{m}^2\cdot\text{K})$ , what yields  $S=175 \text{ m}$ ,  $A=4.6=24 \text{ m}^2$ , and finally  $T_2=50.6 \text{ }^\circ\text{C}$  and  $T_1=33.5 \text{ }^\circ\text{C}$ .

## Reduction to the main dimension (steady state)

We here refer to the simplification of real heat transfer problems when one can reduce the three-dimensional spatial variations and time variation to just one dimension, usually one spatial dimension in the steady state (the spatially-homogeneous, time-changing problem is simpler). By the way, notice how different the bounding conditions in space and time can be; to the richness of 1D-spatial problems, conditions in time usually reduce to an initial value of the function at some time  $t=t_0$ ; that is why almost all numerical methods deal with time in the same simple manner of a time-advancing scheme.

The heat equation (2), in steady state and one spatial dimension, reduces to

$$\frac{1}{r^n} \frac{d}{dr} \left( r^n \frac{dT}{dr} \right) + \frac{\phi(r)}{k} = 0 \quad (15)$$

which has as fundamental solutions, assuming the volumetric energy-source  $\phi$  independent on position, those compiled in Table 2. Particular solutions are obtained by imposing two boundary conditions on the generic  $T(r)$ -expression, as done for the case with no sources (then the heat flow is the same through any distance), and for the case of sources with symmetrical boundary conditions. These solutions teach that one-dimensional temperature profiles are:

- In the absence of internal sources:
  - Linear for planar geometry.
  - Logarithmic for cylindrical geometry.
  - Hyperbolic for spherical geometry.

### Planar, cylindrical, and spherical energy sources, internal or interfacial

With a constant volumetric heat source,  $\phi$  [ $\text{W}/\text{m}^3$ ], a parabolic additional term must be added in all three cases just described, as compiled shown Table 2.

Table 2. Basic solutions for one-dimensional steady heat conduction, i.e. for Eq. (15).

Geometry	Generic $T(r)$	Heat flow	Central temperature*
Planar (slab)	$T(x) = Ax + B - \frac{\phi}{2k}x^2$	$\dot{Q}_{12} \stackrel{\phi=0}{=} k_{12}A \frac{T_1 - T_2}{L_{12}}$	$T_0 \stackrel{T_1=T_2=T_s}{=} T_s + \frac{\phi L^2}{8k}$
Cylindrical	$T(r) = A \ln r + B - \frac{\phi}{4k}r^2$	$\dot{Q}_{12} \stackrel{\phi=0}{=} k_{12}2\pi L \frac{T_1 - T_2}{\ln \frac{R_1}{R_2}}$	$T_0 = T_s + \frac{\phi R^2}{4k}$
Spherical	$T(r) = \frac{A}{r} + B - \frac{\phi}{6k}r^2$	$\dot{Q}_{12} \stackrel{\phi=0}{=} k_{12}4\pi \frac{T_1 - T_2}{\frac{R_1 - R_2}{R_1 R_2}}$	$T_0 = T_s + \frac{\phi R^2}{6k}$

\*Central temperature,  $T_0=T|_{r=0}$ , for a given imposed surface temperature,  $T_s=T|_{r=R}$ ; centred coordinates for slabs, i.e.  $T_0=T|_{x=0}$  and  $T_s=T|_{x=L/2}$ .

One application of these simple solutions may be to the heat flow through slender solid supports between two walls under vacuum, as for a conical stiffener between walls in a dewar flask. The one-dimensional approximation means that the planar frustum cone may be approximated to a spherical-caps frustum cone and, with reference to the cone apex, the cross-section area is  $A(r)=A_1(r/r_1)^2$ , and the temperature profile  $T(r) = T_1 + (\dot{Q}_1^2 / (kA_1))(1/r_1 - 1/r)$ , where  $r_1$  is the radial position of the small face (of area  $A_1$  and temperature  $T_1$ ); notice that the heat flow is independent of  $r$ :  $\dot{Q}(r) = \pi k r_1 r_2 (T_2 - T_1) / (r_2 - r_1)$ , where  $r_2$  is the radial position of the larger face, at temperature  $T_2$ .

If the heat source were interfacial instead of volumetric (i.e.  $\varphi$  [ $\text{W}/\text{m}^2$ ].instead of  $\phi$  [ $\text{W}/\text{m}^3$ ]), and in case of symmetry, the steady solutions would be those presented in Table 3, obtained from (15) as before, but now with  $\phi=0$  and the boundary condition  $\varphi=-kdT/dr|_{R+}$  at the interface, located at  $r=R$ .

Table 3. Steady solutions for one-dimensional heat conduction with a symmetric interfacial heat source  $\varphi$  [ $\text{W}/\text{m}^2$ ]; in all cases  $T(r \leq R)=T_R=\text{constant}$ , and thus  $\dot{Q}(r \leq R) = 0$ .

Geometry	Temperature profile	Heat flux	Heat flow
Planar*	$T(r \geq R) = T_R - \frac{\phi}{k}(r - R)$	$\dot{q}(r \geq R) = \phi$	$\dot{Q}(r \geq R) = A\phi$ (19)
Cylindrical	$T(r \geq R) = T_R - \frac{\phi R}{k} \ln \frac{r}{R}$	$\dot{q}(r \geq R) = \phi \frac{R}{r}$	$\dot{Q}(r \geq R) = 2\pi RL\phi$ (20)
Spherical	$T(r \geq R) = T_R - \frac{\phi R^2}{k} \left( \frac{1}{R} - \frac{1}{r} \right)$	$\dot{q}(r \geq R) = \phi \frac{R^2}{r^2}$	$\dot{Q}(r \geq R) = 4\pi R^2\phi$ (21)

\*The planar case refers to a semi-infinite solid with adiabatic wall at  $r=0$  (or to a slab of thickness  $L$  with two symmetric interfacial dissipation at  $|r|=R < L/2$ ), and  $x$  is often used instead of  $r$  as independent variable (centred midway in a finite slab).

**Exercise 2.** Find the temperature profile in our rod-heated-at-one-end problem, if lateral heat losses to ambient air could be neglected (i.e. by a non-conducting shroud), and the only way out is through the other end.

**Solution.** This is just a planar one-dimensional case, entirely similar to the slab-case in (16) from Table 2, with  $\phi=0$ , which leads to a linear temperature profile and the boundary conditions of our case-study:  $\dot{Q}_0 = -kA(T_0 - T_L)/L = 10$  W and  $-kAdT/dx|_{x=L} = -kA(T_0 - T_L)/L = Ah(T_L - T_\infty)$ , with our data:  $k=200$  W/(m·K),  $A=\pi D^2/4=78 \cdot 10^{-6}$  m<sup>2</sup>,  $h=20$  W/(m<sup>2</sup>·K) and  $T_\infty=15$  °C; i.e. two equations with two unknowns that yield  $T_0=19\ 000$  °C and  $T_L=6300$  °C, a great nonsense that one should have anticipated, since, the basic heat rate at the sink being 20 W/(m<sup>2</sup>·K), one needs a  $\Delta T$  and an active surface  $A$ , satisfying  $A\Delta T = \dot{Q}/h = 0.5$  m<sup>2</sup>·K, and we have just a disc of  $D=1$  cm to evacuate that heat.

**Exercise 3.** Find the maximum temperature difference between the axis and the lateral surface, in our original rod-heated-at-one-end problem.

**Solution.** This difference is expected to be negligible (that is why we approximate rods and fins by one-dimensional heat-transfer problems). This is a cylindrical one-dimensional problem, as in (17), but with coefficient  $A=0$  to avoid the singularity at the axis. We reasoned above ([Exercise 8 in Heat and Mass Transfer](#)) that a lateral heat loss from a rod slice is equivalent to an internal heat sink in the way  $\phi Adx = -hpdx(T - T_\infty)$ , what can be directly substituted in (17):

$$T_0 - T_R = \frac{\phi}{4k} R^2 = \frac{hp(T_R - T_\infty)/A}{4k} R^2 = \frac{h2\pi R(T_R - T_\infty)}{4k\pi R^2} R^2 = \frac{hR}{2k}(T_R - T_\infty) \quad (22)$$

for instance, if the surface temperature is  $T_R=100$  °C, the radial jump from the centre to the periphery would be:

$$T_0 - T_R = \frac{hR}{2k}(T_R - T_\infty) = \frac{20 \cdot 0.01/2}{2 \cdot 200} (373 - 288) = 0.021 \text{ K} \quad (23)$$

i.e., a negligible temperature difference, as expected.

## Multilayer composite walls

Up to now, and in most of what follows on analytical methods, we have focused on simple homogeneous systems. When the system under study comprises several different materials, one must solve each

homogeneous part with unknown interface conditions and match the solutions for temperature and heat flow continuity. For one-dimensional configurations, two cases can be considered:

- Layers in series. This is the normal case where heat flows through a layer and then through the next (i.e. perpendicular to the layers). An example was presented in [Exercise 5 of Heat transfer](#), and another follows here. The general rule is that thermal resistances  $R \equiv \Delta T / \dot{Q}$  add, like electrical resistances ( $R=V/I$ ) in series,  $R=\sum R_i$ ; e.g. for heat flow across planar layers of thickness  $\delta_i$  and conductivities  $k_i$ , the overall conductivity is  $k=\sum \delta_i / \sum (\delta_i / k_i)$ . The ‘Critical radio’ analysis that follows gives additional examples of series resistances for non-planar geometries.
- Layers in parallel. This is the case where heat flows parallel to several superimposed layers. The general rule in this case is that the inverse of thermal resistances  $G \equiv 1/R = \dot{Q} / \Delta T$  add, like for electrical resistances in parallel,  $1/R=\sum (1/R_i)$ ; e.g. for heat flow parallel to several layers of thickness  $\delta_i$  and conductivities  $k_i$ , the overall conductivity is  $k= \sum (\delta_i k_i) / \sum \delta_i$ .

### [Example 1. Dew on window panes](#)

#### Critical radius

An interesting effect in non-planar geometries may occur when adding an 'insulating' layer over a hot thin wire or small sphere, cooled to an ambient fluid; in those cases, it might happen that the increase in heat-transfer area by the additional layer overcomes the effect of a small thermal conductivity of the shroud, giving way to a phenomenon known as critical radius. For instance, for a hot wire of radius  $R$  with a fixed temperature  $T_R$ , exposed to an environment at temperature  $T_\infty$ , with which the convective coefficient is assumed constant,  $h$ , adding an insulating layer of conductivity  $k$  between  $R$  and  $r>R$ :

$$\begin{aligned} \dot{Q}(r \geq R) &= k2\pi L \frac{T_R - T(r)}{\ln \frac{r}{R}} = h2\pi rL(T(r) - T_\infty) = 2\pi L \frac{T_R - T_\infty}{\frac{1}{k} \ln \frac{r}{R} + \frac{1}{rh}} \rightarrow \\ \rightarrow \frac{\partial \dot{Q}}{\partial r} &= 0 \Rightarrow \frac{1}{rk} - \frac{1}{r^2 h} = 0 \Rightarrow r|_{\dot{Q}_{\min}} = \frac{k}{h} \end{aligned} \quad (24)$$

The critical radius for spherical geometry is  $r|_{\dot{Q}_{\min}} = 2k/h$ . As said before, these critical radii only matter when insulating small cylinders ( $R < k/h$ ) and spheres ( $R < 2k/h$ ); e.g., for typical insulators ( $k=0.1$  W/(m·K)) in ambient air ( $h=10$  W/(m<sup>2</sup>·K)), it only matters for wires and pipes smaller than  $k/h=0.1/10=10$  mm.

#### Rods and fins

Many practical heat-transfer problems are not strictly one-dimensional and/or steady, but can be approximated as if they were. A common case is the heat transfer on rods, fins, and other extended surfaces often used to increase the heat-release rate.

Consider a rod protruding from a hot base-plate (Fig. 1) and surrounded by some fluid which has a temperature  $T_\infty$  far from the rod. Assuming the thermal conductivity of the rod to be much greater than that of the fluid, heat would flow basically from the root outside along the rod, with some lateral heat losses to the ambient fluid. Taking a longitudinal element of differential length  $dx$  at some stage  $x$  from



the root, its energy balance is of the form  $mc dT/dt = \sum \dot{Q} = \dot{Q}_x - \dot{Q}_{x+dx} - \dot{Q}_{wet}$ , its mass being  $m = \rho A dx$ ,  $\rho$  the rod-material density,  $A$  rod cross-section area ( $A = \pi D^2/4$  for a circular rod),  $\dot{Q}_x = -kA \partial T / \partial x$ ,  $\dot{Q}_{x+dx} = -kA \left[ \partial T / \partial x + (\partial T^2 / \partial x^2) dx \right]$ , and  $\dot{Q}_{wet} = hp dx (T - T_\infty)$  with  $p$  being the cross-section perimeter ( $p = \pi D$  for a circular rod). The energy balance for that slice is thence:

$$\rho A dx c \frac{\partial T}{\partial t} = -kA \partial T / \partial x + kA \left[ \partial T / \partial x + (\partial T^2 / \partial x^2) dx \right] - hp dx (T - T_\infty)$$

$$\rightarrow \frac{\rho c}{k} \frac{\partial T}{\partial t} = \frac{\partial T^2}{\partial x^2} - \frac{hp}{kA} (T - T_\infty) \xrightarrow{\text{steady}} \frac{dT^2}{dx^2} = m^2 (T - T_\infty), \quad m \equiv \sqrt{\frac{hp}{kA}} \quad (25)$$

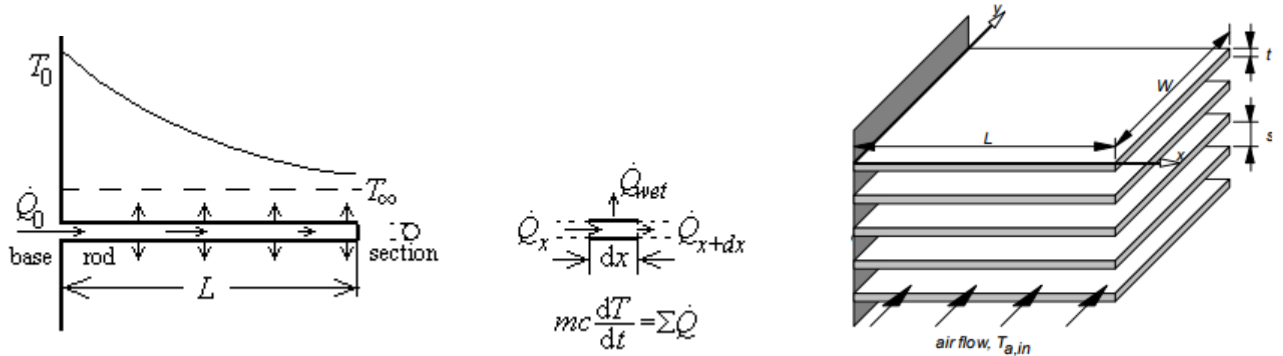


Fig. 1. a) Sketch of heat flow in a circular rod protruding from a hot base-plate and surrounded by a fluid, and a generic longitudinal differential element  $dx$ . b) A set of planar fins.

A physical interpretation of the non-dimensional parameter  $mL$  is that it relates heat flow by convection in an isothermal fin,  $\dot{Q}_{conv} = pLh(T_0 - T_\infty)$ , to heat flow by conduction along a laterally-insulated fin,  $\dot{Q}_{cond} = kA(T_0 - T_\infty)/L$ ; i.e. by substitution,  $(mL)^2 = hp/(kA) = \dot{Q}_{conv} / \dot{Q}_{cond}$ .

Solving the differential equation (25) in the steady state is straightforward, yielding an exponential function  $T(x) = A \exp(mx) + B \exp(-mx)$ , often set in terms of hyperbolic functions, whose coefficients are obtained by establishing the appropriate boundary conditions. For instance, for given root temperature ( $T_0$ ), and adiabatic end ( $\dot{Q}_L \equiv -kA dT/dx|_{x=L} = 0$ ), the solution is  $(T(x) - T_\infty)/(T_0 - T_\infty) = \cosh(m(L-x))/\cosh(mL)$ , and the heat flow at the root is  $\dot{Q}_0 = (T_0 - T_\infty) \sqrt{phkA} \tanh(mL)$ . Often, a fin efficiency is defined as the ratio of heat evacuated by the fin divided by the heat it would evacuate if all the fin was at the root temperature, i.e.  $\eta \equiv \dot{Q}_0 / [pLh(T_0 - T_\infty)] = \tanh(mL)/(mL)$ , although it is a poor concept (it is just the corollary that the more conductive the fin, the best), without any indication of how to improve fin geometry. Another possibility is defining fin efficiency as the heat flow with fin, divided by the heat flow without fin (i.e. only by convection at the root area), but it only shows that the larger the fin, the better. For a given root area available, a more interesting design consideration is the optimum number of fins, and fin geometry; total heat flow is proportional to the number of fins, but if placed too close, the assumption of independency is lost: the fluid flow in between becomes more difficult and the convective coefficient decreases.

It is not difficult to extend the previous analysis to other fin configurations. Table 4 presents the most important cases. For instance, the effect of a uniform heat release of volumetric power  $\phi$  [ $W/m^3$ ] along the fin (e.g. to model a one-dimensional heater) can easily be added to (25); e.g., the solution of

$d^2T/dx^2=m^2(T-T_\infty)+\phi/k$  for Case 1 in Table 4 changes from  $(T-T_\infty)/(T_0-T_\infty)=\cosh(m(L-x))/\cosh(mL)\equiv f$  to  $(T-T_\infty)/(T_0-T_\infty)=f+\phi(1-f)/(km^2(T_0-T_\infty))$ . For more general configurations, as non-uniform heat-source distributions  $\phi(x)$ , slowly-varying cross-section area  $A(x)$ , variation on material properties (e.g.  $k(x)$ ), and so on, the solution of the differential equation gets so complicated that it is wiser to resort to numerical simulation.

Table 4. Some analytical solutions for the heat equation (25) along a rod, bar or wire, immersed in a fluid.

Case	Conditions	Temperature profile	End results
1	$T(0)=T_0$ $\left.\frac{dT}{dx}\right _{x=L}=0$	$\frac{T(x)-T_\infty}{T_0-T_\infty}=\frac{\cosh[m(L-x)]}{\cosh(mL)}$	$\frac{\dot{Q}_0}{(T_0-T_\infty)\sqrt{phkA}}=\tanh(mL)$ $\dot{Q}_L=0$
2	$T(0)=T_0$ $T(L)=T_L$	$\frac{T(x)-T_\infty}{T_0-T_\infty}=\frac{\sinh[m(L-x)]}{\sinh(mL)}+$ $+\frac{T_L-T_\infty}{T_0-T_\infty}\frac{\sinh(mx)}{\sinh(mL)}$	$\frac{\dot{Q}_0}{(T_0-T_\infty)\sqrt{phkA}}=\frac{1}{\tanh(mL)}-\frac{T_L-T_\infty}{T_0-T_\infty}\frac{1}{\sinh(mL)}$ $\frac{\dot{Q}_L}{(T_0-T_\infty)\sqrt{phkA}}=\frac{1}{\sinh(mL)}-\frac{T_L-T_\infty}{T_0-T_\infty}\frac{1}{\tanh(mL)}$
3	$\dot{Q}(0)=\dot{Q}_0$ $\dot{Q}(L)=0$	$\frac{T(x)-T_\infty}{\dot{Q}_0/\sqrt{phkA}}=\frac{\cosh[m(L-x)]}{\sinh(mL)}$	$\frac{T(0)-T_\infty}{\dot{Q}_0/\sqrt{phkA}}=\frac{1}{\tanh(mL)}$ $\frac{T(L)-T_\infty}{\dot{Q}_0/\sqrt{phkA}}=\frac{1}{\sinh(mL)}$
4	$\dot{Q}(0)=\dot{Q}_0$ $\dot{Q}(L)=\dot{Q}_L$	$\frac{T(x)-T_\infty}{\dot{Q}_0/\sqrt{phkA}}=\frac{\cosh[m(L-x)]}{\sinh(mL)}+$ $+\frac{\dot{Q}_L}{\dot{Q}_0}\frac{\cosh(mx)}{\sinh(mL)}$	$\frac{T(0)-T_\infty}{\dot{Q}_0/\sqrt{phkA}}=\frac{1}{\tanh(mL)}+\frac{\dot{Q}_L}{\dot{Q}_0}\frac{1}{\sinh(mL)}$ $\frac{T(L)-T_\infty}{\dot{Q}_0/\sqrt{phkA}}=\frac{1}{\sinh(mL)}+\frac{\dot{Q}_L}{\dot{Q}_0}\frac{1}{\tanh(mL)}$

The combined problem of a fin with convection ( $h$  [W/(m<sup>2</sup>·K)]) and internal heat release ( $\phi$  [W/m<sup>3</sup>]), both uniform, allows close analytical solutions too; e.g. for a fin of length  $L$ , with equal temperature at both ends, kept constant, the differential formulation with  $x$ -origin centred is:

$$\frac{dT^2}{dx^2}=m^2(T-T_\infty)+\frac{\phi}{k}, \quad \text{with } T|_{x=\pm\frac{L}{2}}=T_0 \text{ and } m\equiv\sqrt{\frac{hp}{kA}} \quad (26)$$

is:

$$\frac{T(x)-T_\infty}{T_0-T_\infty}=\frac{\cosh[mx]}{\cosh\left(\frac{mL}{2}\right)}+\frac{1}{T_0-T_\infty}\frac{\phi}{m^2k}\left(1-\frac{\cosh[mx]}{\cosh\left(\frac{mL}{2}\right)}\right) \quad (27)$$

where it can be checked that, for  $\phi=0$ , (27) recovers Case 2 of Table 4 (for equal ends), and for  $h=0$  ( $m=0$ ), (27) recovers the Planar case of Table 2 (for equal ends with centred origin).

**Exercise 4.** Find the steady temperature profile in our rod-heated-at-one-end problem.

Solution. This is just case 3 in Table 4, here re-elaborated as an exercise. We consider this problem to be one-dimensional and planar for heat conduction (along the axial direction), with internal heat sinks to account for the actual lateral heat losses by convection (i.e. with  $\phi A dx = -hp dx (T - T_\infty)$ ,  $p$  being the cross-section perimeter and  $A$  the cross-section area), and apply (3) to an infinitesimal slice:

$$\rho c A dx \frac{\partial T}{\partial t} = k A dx \nabla^2 T - hp dx (T - T_\infty) \xrightarrow{t \rightarrow \infty} 0 = \frac{d^2 T}{dx^2} - \frac{hp}{kA} (T - T_\infty) \quad (28)$$

with:

$$\dot{Q}_0 = -kA \left. \frac{dT}{dx} \right|_{x=0} \quad \& \quad 0 = -kA \left. \frac{dT}{dx} \right|_{x=L} \Rightarrow T(x) = T_\infty + \frac{\dot{Q}_0}{mkA} \frac{\cosh(m(L-x))}{\sinh(mL)} \quad (29)$$

where  $m \equiv \sqrt{hp/(kA)}$ ,  $h$  being the convective coefficient,  $p$  the perimeter of the rod cross-section ( $\pi D$  if circular),  $A$  the cross-section area ( $\pi D^2/4$  if circular), and  $L$  the rod length.

**Exercise 5.** A method to measure the thermal conductivity of non-metal slabs, consists on having a small copper disc (like a coin) lodged at level into a high-insulating wall, with thermocouples at both sides of the copper disc. When a thin sample slab (a plate), is sandwiched between a heat source at constant temperature (e.g. with boiling water), and the mentioned 'heat-meter', a transient heat-up takes place on the copper disc. If the temperature profile within the sample plate is assumed linear as in a quasi-steady state, and the temperature within the copper disc is uniform, find a relationship between the thermal conductivity of the sample, and the measured temperatures.

Solution. The energy balance of the copper disc yields:

$$\begin{aligned} m_{\text{Cu}} c_{\text{Cu}} \frac{dT_{\text{Cu}}}{dt} &= k_{\text{sample}} A_{\text{Cu}} \frac{T_0 - T_{\text{Cu}}}{L_{\text{sample}}} \rightarrow \frac{d(T_0 - T_{\text{Cu}})}{T_0 - T_{\text{Cu}}} = \frac{-k_{\text{sample}} A_{\text{Cu}}}{m_{\text{Cu}} c_{\text{Cu}} L_{\text{sample}}} dt \rightarrow \\ \rightarrow \frac{T_0 - T_{\text{Cu}}(t)}{T_0 - T_{\text{Cu,initial}}} &= \exp\left(\frac{-k_{\text{sample}} A_{\text{Cu}}}{m_{\text{Cu}} c_{\text{Cu}} L_{\text{sample}}} t\right) \end{aligned} \quad (30)$$

which allows the computation of the thermal conductivity of the sample,  $k_{\text{sample}}$ , by a simple linear fitting of the logarithm of copper-temperatures versus time.

### Heat source moving at steady state along a rod

In some heat-transfer applications, there is a relative motion between the material and the heat source. Consider a long and thin circular rod with a single coaxial heating-coil, as in Fig. 2a; the solution to this problem can also be applied to the case of a long rod partially within a semi-infinite furnace, as in Fig. 2b.

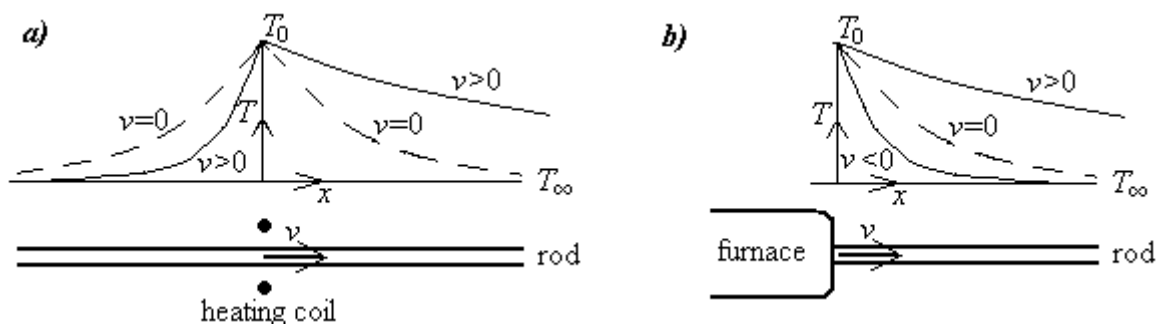


Fig. 2. Steady temperature profile in a rod moving with velocity  $v$  past a heating coil (a), or relative to a furnace (b), with heat transfer by conduction along the rod and by convection to an ambient fluid. Dotted lines ( $v=0$ ) corresponds to no relative motion, and  $v<0$  to the rod entering the furnace.

The heat equation (2), for the steady case of a rod moving past a heating coil, and the corresponding boundary conditions, may be set like that:

$$\left. \begin{aligned} 0 &= k \frac{d^2 T}{dx^2} - \frac{hp(T - T_\infty)}{A} + \rho cv \frac{dT}{dx} \\ \text{for } x < 0 & \quad T|_{x=-\infty} = T_\infty, \quad T|_{x=0} = T \\ \text{for } x > 0 & \quad T|_{x=0} = T_0, \quad T|_{x=\infty} = T_\infty \end{aligned} \right\} \quad (31)$$

which has the solution:

$$\frac{T - T_\infty}{T_0 - T_\infty} = \exp \left[ \frac{-xv}{2a} \left( 1 \pm \sqrt{1 + \left( \frac{2am}{v} \right)^2} \right) \right], \quad \dot{Q}_0 = kA(T_0 - T_\infty) \frac{v}{2a} \left( 1 \pm \sqrt{1 + \left( \frac{2am}{v} \right)^2} \right) \quad (32)$$

where the ' $\pm$ ' means that '+' should be taken for  $x > 0$  and '-' applies for  $x < 0$ , and, as before,  $m \equiv \sqrt{hp/(kA)}$ ,  $h$  being the convective coefficient,  $p$  the perimeter of the rod cross-section ( $\pi D$  if circular), and  $A$  the cross-section area ( $\pi D^2/4$  if circular). It can be verified that, in the limit of no relative motion ( $v=0$ ), there heat flow in (32) becomes  $|\dot{Q}_0| = (T_0 - T_\infty) \sqrt{phkA}$  at each side of the origin, corresponding to case 1 of Table 4 for very long rods ( $mL \gg 1$ ).

### Reduction by dimension similarity (unsteady state)

Reduction by dimension similarity occurs when a partial differential equation can be converted to an ordinary differential equation in a combined variable, due to lack of characteristic lengths and times. For instance, for  $v \neq 0$ , the partial differential equation (PDE) (3) transforms to an ordinary differential equation (ODE):

$$\frac{1}{r^n} \frac{\partial}{\partial r} \left( r^n \frac{\partial T}{\partial r} \right) - \frac{1}{a} \frac{\partial T}{\partial t} = 0 \xrightarrow{\eta(r,t) \equiv \frac{r}{\sqrt{4at}}} \frac{d^2 T(\eta)}{d\eta^2} + \left( 2\eta + \frac{n}{\eta} \right) \frac{dT(\eta)}{d\eta} = 0 \quad (33)$$

which can be solved in general in terms of hypergeometric functions, and, in particular, for each space dimension, in terms of the error function,  $\text{erf}(x) = \left( 2/\sqrt{\pi} \right) \int_0^x \exp(-x^2) dx$ , and the exponential integral,  $\text{Ei}(x) \equiv \int_{-\infty}^x [\exp(x)/x] dx$ , as detailed below.

- Planar solutions. Solving (33) with  $n=0$  yields  $T(\eta) = A + B \text{erf}(\eta)$ , but, because of the linearity of  $a d^2 T/dx^2 - dT/dt = 0$ , not only that function but its partial derivatives to any order in  $x$  and  $t$  will be solutions to (33), and in particular  $\partial \text{erf}(\eta)/\partial x$  and  $\partial \text{erf}(\eta)/\partial t$ , namely:

$$\left. \begin{aligned} T(x,t) &= A + B \operatorname{erf}\left(\frac{x}{\sqrt{4at}}\right) \\ T(x,t) &= \frac{A}{\sqrt{t}} \exp\left(\frac{-x^2}{4at}\right) \\ T(x,t) &= \frac{A}{t} \frac{x}{\sqrt{4at}} \exp\left(\frac{-x^2}{4at}\right) \end{aligned} \right\} \quad (34)$$

- Cylindrical solutions. Solving (33) with  $n=1$  yields  $T(\eta)=A+BEi(-\eta^2)$ , where  $Ei(x)$  is the exponential integral, but now only its partial derivatives in  $t$  will be solutions too; in particular:

$$\left. \begin{aligned} T(r,t) &= A + B Ei\left(\frac{-r^2}{4at}\right) \\ T(r,t) &= \frac{A}{t} \exp\left(\frac{-r^2}{4at}\right) \end{aligned} \right\} \quad (35)$$

- Spherical solutions. Solving (33) with  $n=2$  yields  $T(\eta) = A + B\left(\sqrt{\pi}\operatorname{erf}(\eta) + \exp(-\eta^2)/\eta\right)$ , but again only its partial derivatives in  $t$  will be solutions too; in particular:

$$\left. \begin{aligned} T(r,t) &= A + B \left[ \sqrt{\pi} \operatorname{erf}\left(\frac{r}{\sqrt{4at}}\right) + \exp\left(\frac{-r^2}{4at}\right) / \left(\frac{r}{\sqrt{4at}}\right) \right] \\ T(r,t) &= \frac{A}{r\sqrt{t}} \exp\left(\frac{-r^2}{4at}\right) \end{aligned} \right\} \quad (36)$$

### Energy deposition in unbounded media

A most basic application of similarity solutions is the temperature field due to a thermal pulse in an unbounded medium, i.e. the instantaneous release of an amount of energy  $Q$  at the origin; in mathematical terms, this can be formulated in two different ways, here shown for the planar case:

- As a singular initial-value problem in temperature without sources:

$$\left. \begin{aligned} \text{At } t=0 \quad T(x,t) &= T_\infty + \frac{Q}{\rho c} \delta(x,t) \\ \text{For } t > 0 \quad \frac{\partial^2 T(x,t)}{\partial x^2} - \frac{1}{a} \frac{\partial T(x,t)}{\partial t} &= 0 \end{aligned} \right\} \quad (37)$$

- As a singular-source regular problem in temperature:

$$\left. \begin{aligned} \text{For } \forall(x,t) \quad \frac{\partial^2 T(x,t)}{\partial x^2} + \frac{\phi(x,t)}{k} - \frac{1}{a} \frac{\partial T(x,t)}{\partial t} &= 0 \\ \text{with } \phi(x,t) &= Q \delta(x,t) \end{aligned} \right\} \quad (38)$$

The solution can be expressed in a compact form valid for multiple geometries:

$$T(r,t) = T_\infty + \frac{Q \exp\left(\frac{-r^2}{4at}\right)}{\rho c (4\pi at)^{\frac{1+n}{2}}}, \quad T(0,t) = T_\infty + \frac{Q}{\rho c (4\pi at)^{\frac{1+n}{2}}}, \quad \int_V (T - T_\infty) dV = \frac{Q}{\rho c} \quad (39)$$

where the last integral extends to the whole space in the variable considered (one-dimensional, two-dimensional, or three-dimensional volume), according to the  $n$ -value:

- $n=0$  for the planar geometry, where  $r$  should be understood as the  $x$ -coordinate, and  $Q$  is the energy released at  $x=0$  and  $t=0$  per unit area.
- $n=1$  for the cylindrical geometry, where  $Q$  is the energy released per unit length, and the
- $n=2$  for the spherical geometry, where  $Q$  is the total energy released initially at the centre.

An example of the temperature profiles obtained is presented in Fig. 3 for the configuration detailed in the exercise following.  $T_\infty$  is the initial temperature of the solid (and the value at  $x \rightarrow \infty$  for any time, or at  $t \rightarrow \infty$  for any  $x$ ). Notice that at a given distance  $x$ , temperature attains a maximum value in time ( $\partial T / \partial t = 0$ ) after a lapse  $\Delta t = x^2 / (2a)$  from the pulse; i.e. the initial pulse (at  $x=0$ ) travels at a speed  $dx/dt = \sqrt{a/(2t)}$ , decreasing in amplitude with time too. A time  $t$  after the pulse, the maximum is at  $x = \sqrt{2at}$  and values  $T_{\max} = Q / (\rho c \sqrt{4\pi e a t})$ . It happens that, at a given time, this  $T_{\max}$  (taking place at  $x = \sqrt{2at}$ ) is simply related to the temperature at  $x=0$  by  $T_{\max} = T(0,t) / e^{1/2} = 0.61 \cdot T(0,t)$  (mind that  $T(x,t)$  always decreases with  $x$ , but has a maximum with  $t$ ).

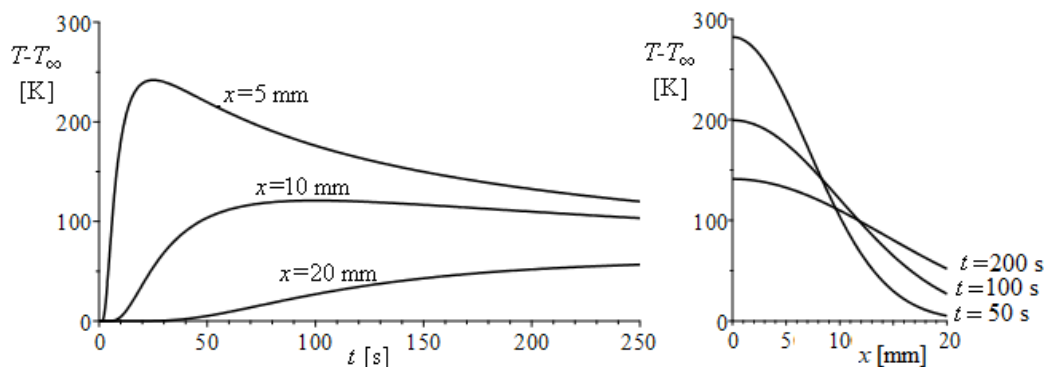


Fig. 3. a) Temperature evolution at three points in a semi-infinite slab with a heat pulse at  $x=0$ . b) Spatial temperature profiles at three instants in time. (Exercise 6.)

**Exercise 6.** For an analysis of the temperature field in a brake pad of thickness  $L=0.02$  m (the other dimensions being much larger), when suddenly rubbed on one face, consider an instantaneous deposition of  $Q=10$  MJ/m<sup>2</sup> on one side of a slab of conductivity  $k=1$  W/(m·K), density  $\rho=2000$  kg/m<sup>3</sup>, thermal capacity  $c=1000$  J/(kg·K), and no heat losses to the ambient, and find the temperature history in the middle of the slab. Formulate the problem as an unbounded medium, and quantify the constraints imposed by this simplification.

**Solution.** The general solution for unbounded media has been given in (39), here to be applied to the planar case,  $n=0$ ; i.e., at a point  $x_1$ ,  $T(t)$  becomes:

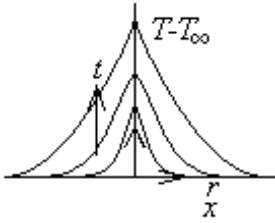
$$T(x,t) - T_\infty = \frac{Q \exp\left(\frac{-x^2}{4at}\right)}{\rho c \sqrt{4\pi at}} = \frac{10^7 \exp\left(\frac{-x_1^2}{4 \cdot 0.5 \cdot 10^{-6} \cdot t}\right)}{2000 \cdot 1000 \sqrt{4\pi \cdot 0.5 \cdot 10^{-6} \cdot t}} \quad (40)$$

where  $a=k/(\rho c)=1/(2000 \cdot 1000)=0.5 \cdot 10^{-6}$  m<sup>2</sup>/s. In Fig. 3a above, the temperature evolution is plotted for the desired point  $x_1=L/2=0.01$  m, and for two other locations, at half and double distance to the heated surface; notice that the last location,  $x=0.02$  m, is precisely the end of the slab, which was to be adiabatic, and is incompatible with the approximation of semi-infinite-thick slab (this helps to quantify the validity of the unbounded solution; in our case, Fig. 3 shows that it takes about 50 s for the back of the pad to notice the heating (at that time the rubbed surface has cooled to  $T(0)<300$  K above the initial temperature  $T_\infty$ ). Notice that the temperature evolution at  $x=0$ ,  $T(0,t)$ , is not valid for very short times (in practice, the rubbing will take some time, say a few seconds). The temperature evolution at the middle point deduced with the unbounded model may be valid for the first few minutes.

The instantaneous deposition of energy studied above, can be extended to several other problems where the deposition is not instantaneous and at a point, but extended in time or space, by time integration or space integration of infinitesimal instantaneous depositions at different times or places, respectively, with the results compiled in Table 5, where the original case (35) has been also included. Some of these solutions are the most used and accurate methods to measure thermal properties of materials, either in continuous heat release mode (e.g. [heating needle](#)), or as a heat pulse (e.g. using two small nearby thermistors, say 0.5 mm in diameter separated  $r=5$  mm, the time it takes for a heat pulse, say of 0.1 W during 1 s, in one resistor to reach the other one is, from (39),  $\Delta t=r^2/(6a)$ , with a  $\Delta T_{\max}=(\epsilon\pi)^{3/2}Q/(8k\Delta t^{3/2})=0.005 \cdot Q/(k\Delta t^{3/2})$ , which allows determining  $a$ ,  $k$ , and  $c=k/(\rho a)$ .

Table 5. Some analytical solutions for the unsteady heat equation in unbounded media (31);  $a=k/(\rho c)$ .

Problem	Solution	Notes
1. Instantaneous point-source deposition, one-, two-, tri- dimensional with $\int_V (T - T_\infty) dV = \frac{Q}{\rho c}$	$T(r,t) = T_\infty + \frac{Q \exp\left(\frac{-r^2}{4at}\right)}{\rho c (4\pi at)^{\frac{1+n}{2}}}$ $T(0,t) = T_\infty + \frac{Q}{\rho c (4\pi at)^{\frac{1+n}{2}}}$	Planar case: $n=0$ and $Q$ [J/m <sup>2</sup> ]. Cylindr. case: $n=1$ and $Q$ [J/m]. Spherical case: $n=2$ and $Q$ [J]. $t=0$ , Delta(x). $t>0$ , Gauss bell.
2. Continuous point-source deposition, one-, two-, tri- dimensional with $\int_V (T - T_\infty) dV = \frac{\dot{Q}t}{\rho c}$	Planar: $\frac{T(x,t) - T_\infty}{\frac{\dot{Q}}{2k} x} = \frac{\exp(-\eta^2)}{\sqrt{\pi}\eta} + \text{erf}(\eta) - \text{sgn}(\eta)$	$\dot{Q}$ =Heaviside( $t$ ) at $x=0$ Planar $\dot{Q}$ [W/m <sup>2</sup> ], with $\eta = \frac{x}{\sqrt{4at}}$ Axial $\dot{Q}$ [W/m], with



Axial ( $r>0$ ): 
$$\frac{T(r,t)-T_\infty}{\frac{\dot{Q}}{4\pi\rho ca}} = -\text{Ei}(-\eta^2)$$

$$\eta \equiv \frac{r}{\sqrt{4at}}$$

$$\dot{Q} = 4\pi k \frac{\partial T}{\partial t} \Big|_{r^2 \ll 4at}$$

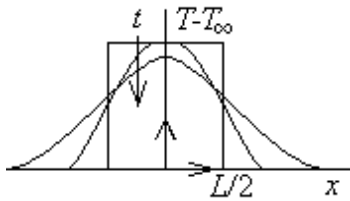
Notice that  $\text{Ei}(-\eta^2)$  is singular at  $\eta=0$ , but, for  $\eta \ll 1$  ( $r \ll \sqrt{4at}$ ),  $-\text{Ei}(-\eta^2) \rightarrow -\gamma - \ln(\eta^2)$ , with  $\gamma=0.577$ , and  $\partial \ln(\eta^2)/\partial t = -1/t$ , independent of  $r$ .

Point  $\dot{Q}$  [W], with

$$\eta \equiv \frac{r}{\sqrt{4at}}$$

Point source: 
$$\frac{T(r,t)-T_\infty}{\frac{\dot{Q}}{4\pi\rho ca r}} = \text{erfc}(-\eta)$$

3. Instantaneous finite line-source, one-dimensional deposition of initial width  $L$



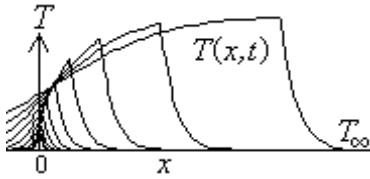
$$\frac{T(x,t)-T_\infty}{\frac{\dot{Q}}{2\rho cL}} = \left( \text{erf}\left(\frac{\frac{L}{2}+x}{\sqrt{4\pi at}}\right) + \text{erf}\left(\frac{\frac{L}{2}-x}{\sqrt{4\pi at}}\right) \right)$$

$$\frac{T(0,t)-T_\infty}{\frac{\dot{Q}}{\rho cL}} = \text{erf}\left(\frac{L}{4\sqrt{at}}\right)$$

$t>0$ .

Tends to a point-source (Gauss bell) for  $t \rightarrow \infty$

4. Continuous planar-source deposition moving at speed  $V$  and lasting from  $t=0$  (at  $x=0$ ) to  $t_1$ .

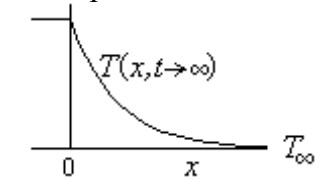


$$\frac{T(x,t)-T_\infty}{2\rho cV} \xrightarrow[t \rightarrow \infty]{\text{moving axes}} \begin{cases} -x < 0 \rightarrow 1 \\ -x \geq 0 \rightarrow \exp\left(\frac{-xV}{a}\right) \end{cases}$$

$$\frac{T(0,t)-T_\infty}{2\rho cV} \xrightarrow[\text{fix axes}]{} 1 - \exp\left(\frac{V^2 t}{a}\right) \text{erfc}\left(\sqrt{\frac{V^2 t}{a}}\right)$$

$\dot{Q}$  [W/m<sup>2</sup>].

$T(x,t)$  has not a simple form, but  $T(x,t \rightarrow \infty)$  in moving axes has a plot like this:



$T(0,t)$  (i.e. where deposition starts) is in fixed axes.

5. Continuous line-source deposition moving at speed  $V$ . Steady state.



$$\frac{T(x,y)-T_\infty}{2\pi k} = \exp\left(\frac{Vx}{2a}\right) K_0\left(\frac{Vr}{2a}\right)$$

$$\frac{T(x,y)-T_\infty}{2\pi k} \xrightarrow{x \gg y} \sqrt{\frac{\pi a}{Vx}} \left(1 - \frac{Vy^2}{4ax}\right)$$

$\dot{Q}$  [W/m].

$K_0$  is the modified Bessel function of the second kind.

$$r = \sqrt{x^2 + y^2}$$

6. Continuous point-source deposition moving at speed  $V$ . Steady state.



$$\frac{T(x,y,z)-T_\infty}{4\pi kr} = \exp\left(\frac{-V(r-x)}{2a}\right)$$

$$\frac{T(x,y,z)-T_\infty}{4\pi kx} \xrightarrow{x \gg \sqrt{y^2+z^2}} \exp\left(\frac{-V(y^2+z^2)}{4ax}\right)$$

$\dot{Q}$  [W].

$$r = \sqrt{x^2 + y^2 + z^2}$$

7. Infinite rod moving at speed  $V$  in ( $V<0$ ) or out ( $V>0$ ) of a furnace.

$$\frac{T(x)-T_f}{T_0-T_f} \xrightarrow{x < 0} \exp\left(\frac{Vx}{2a} \left(1 + \sqrt{1 + \left(\frac{2am}{V}\right)^2}\right)\right)$$

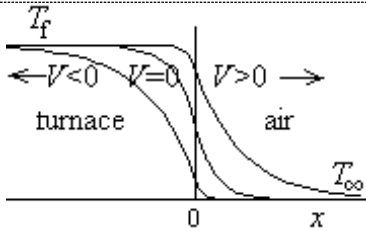
The furnace is at  $x<0$  and  $T_f$ .

$T_0$  is the rod temperature at the mouth.

The outside fluid is at  $x>0$  and  $T_\infty$ .

The convective coefficient  $h$  is the same inside and outside..



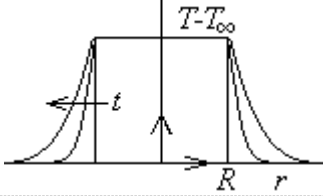


$$\frac{T(x) - T_{\infty}}{T_0 - T_{\infty}} = \exp\left(\frac{Vx}{2a} \left(1 - \sqrt{1 + \left(\frac{2am}{V}\right)^2}\right)\right)$$

$$T_0 = \frac{T_f + T_{\infty}}{2} - \frac{T_f - T_{\infty}}{2} \frac{V}{\sqrt{V^2 + 4a^2m^2}}$$

$m \equiv \sqrt{\frac{hp}{kA}}$ , with  $p$  and  $A$  being the perimeter and area of the rod cross-section.

### 8. Continuous spherical-source kept at fixed- $T$ .



$$\frac{T(r,t) - T_{\infty}}{T_R - T_{\infty}} = \frac{R}{r} \operatorname{erfc}\left(\frac{r-R}{\sqrt{4at}}\right)$$

Only valid for  $r > R$ .

The heat supplied to the sphere must be controlled to match

$$\dot{Q}(t) = k4\pi R^2 (T_R - T_{\infty}) \left(\frac{1}{R} + \frac{1}{\sqrt{\pi at}}\right)$$

### Thermal contact in semi-infinite media

Another important kind of thermal problems where similarity in the variables make them amenable to analytical solution is a sudden change in the boundary condition of semi-infinite bodies, which can be applied to practical geometries of finite thickness  $L$  for short-enough times, because for  $t \ll L^2/a$  ( $Fo \ll 1$ ) the solid can be supposed semi-infinite.

For instance, for the sudden thermal change in a the face of a planar semi-infinite body (as developed in [Exercise 8 in the Introduction](#)), the transient temperature profiles are given by (34). The following example (Fig. 4) illustrates an imposed-convection case.

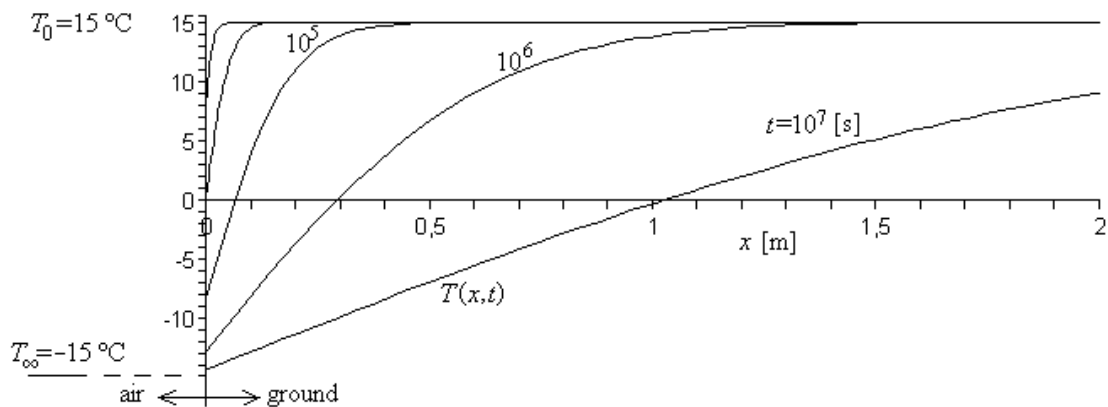


Fig. 4. Temperature profiles at several time intervals in a solid material initially at 15 °C, suddenly exposed to air at -15 °C with constant convective coefficient.

**Exercise 7.** Find for how long air-freezing temperatures of -10 °C can be tolerated, without freezing penetration to 1 m depth in soil, assuming and initial  $T$ -field at 15 °C, a sudden change in air temperature from 15 °C to -10 °C (with no further variation), a convective coefficient of  $h=10$  W/(m<sup>2</sup>·K), and the soil having  $\rho=2000$  kg/m<sup>3</sup>,  $c=2000$  J/(kg·K),  $k=0.5$  W/(m·K), and without freezing effects.

**Solution.** Applying the initial and boundary conditions for the soil, to the general solution (34), one gets:

$$T = c_1 + c_2 \operatorname{erf}(\eta), \quad \text{with } -k \frac{\partial T}{\partial x} \Big|_{x=0} = h(T_\infty - T|_{x=0}) \quad \& \quad T(x,0) = T_0 \Rightarrow$$

$$\Rightarrow T(x,t) = T_0 + (T_\infty - T_0) \left[ \operatorname{erfc}\left(\frac{x}{2\sqrt{at}}\right) - \exp\left(\frac{hx}{k} + \frac{h^2 at}{k^2}\right) \operatorname{erfc}\left(\frac{x}{2\sqrt{at}} + \frac{h\sqrt{at}}{k}\right) \right] \quad (41)$$

and the desired time-period is obtained by solving (41) for  $T(x,t)=0$  °C (water freezing) at  $x=1$  m, with  $T_0=15$  °C and  $T_\infty=-15$  °C, an implicit equation that yields  $t=9.7 \cdot 10^6$  s (i.e. some 110 days). Figure 4 shows the temperature profile at several times.

Another important application of similarity solutions is the evaluation of the contact temperature when two solids at different temperature get into contact.

Let solid A extend from  $x=0$  to  $+\infty$ , initially at  $T_A$ , and solid B extend from  $x=0$  to  $-\infty$ , initially at  $T_B$ , and let  $T_0$  be the contact temperature (at  $x=0$ ). Applying the initial and boundary conditions to the general solution (34) for solid A:

$$T = c_1 + c_2 \operatorname{erf}(\eta), \quad \text{with } T(x,0) = T_A \quad \& \quad T(0,t) = T_0 \Rightarrow T_A(x,t) = T_0 + (T_A - T_0) \operatorname{erf}\left(\frac{x}{2\sqrt{a_A t}}\right)$$

$$\text{with } \dot{q}_A = -k_A \frac{\partial T_A}{\partial x} \Big|_{x=0} = -\frac{k_A (T_A - T_0)}{\sqrt{\pi a_A t}} \quad (42)$$

whereas for solid B:

$$T = c_1 + c_2 \operatorname{erf}(\eta), \quad \text{with } T(x,0) = T_B \quad \& \quad T(0,t) = T_0 \Rightarrow T_B(x,t) = T_0 + (T_B - T_0) \operatorname{erf}\left(\frac{-x}{2\sqrt{a_B t}}\right)$$

$$\text{with } \dot{q}_B = -k_B \frac{\partial T_B}{\partial x} \Big|_{x=0} = \frac{k_B (T_B - T_0)}{\sqrt{\pi a_B t}} \quad (43)$$

Now, the energy balance at the interface (continuity of heat flux) implies:

$$\frac{k_A (T_A - T_0)}{\sqrt{\pi a_A t}} + \frac{k_B (T_B - T_0)}{\sqrt{\pi a_B t}} = 0 \Rightarrow T_0 = \frac{T_A \sqrt{k_A \rho_A c_A} + T_B \sqrt{k_B \rho_B c_B}}{\sqrt{k_A \rho_A c_A} + \sqrt{k_B \rho_B c_B}} \quad (44)$$

where the parameter  $\sqrt{k\rho c}$  is called thermal effusivity,  $e$  (or thermal inertia,  $i$ ), with units of  $\text{J}/(\text{m}^2 \cdot \text{K} \cdot \text{s}^{1/2})$  or  $\text{kg}/(\text{K} \cdot \text{s}^{5/2})$ . The following exercise presents a simple application.

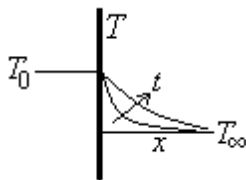
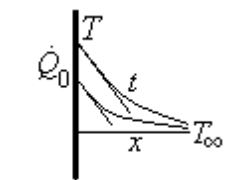
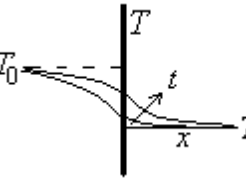
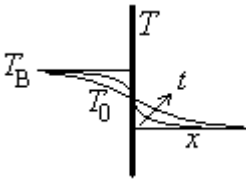
**Exercise 8.** Find the contact temperature between a bare foot and a floor at 10 °C, for the case of wooden floor and for the case of ceramic floor.

**Solution.** For our flesh we estimate its thermal data by approximation to those of leather in [Solid thermal data](#):  $k=0.4$  W/(m·K),  $\rho=1000$  kg/m<sup>3</sup>,  $c=1500$  J/(kg·K), what yields  $\sqrt{k\rho c} = \sqrt{0.4 \cdot 1000 \cdot 1500} = 770$  kg·K<sup>-1</sup>·s<sup>-5/2</sup>. For wood, a look-up in the same table (for oak wood) gives:  $\sqrt{k\rho c} = \sqrt{0.17 \cdot 750 \cdot 2400} = 550$  kg·K<sup>-1</sup>·s<sup>-5/2</sup>, and for ceramic tiles (with marble data):  $\sqrt{k\rho c} = \sqrt{2.6 \cdot 2700 \cdot 880} = 2500$  kg·K<sup>-1</sup>·s<sup>-5/2</sup>, so that, if we assume our body at 37 °C (feet

are always a few degrees colder) and the floor at 10 °C, the skin in contact with wood will face (nearly instantaneously) a temperature of (8):  $(37 \cdot 770 + 10 \cdot 550) / (770 + 550) = 22$  °C, whereas in contact with ceramic tiles will have  $(37 \cdot 770 + 10 \cdot 2500) / (770 + 2500) = 16.4$  °C, what makes a great difference (we may feel variations in our skin temperature of a few tenths of a degree!).

A compilation of similarity solutions for semi-infinite bodies is presented in Table 6.

Table 6. Some self-similar analytical solutions for the unsteady heat equation in semi-infinite bodies (31).

Problem	Solution	Notes
<p>1. Step jump in surface temperature</p> 	$\frac{T(x,t) - T_\infty}{T_0 - T_\infty} = \operatorname{erfc}\left(\frac{x}{2\sqrt{at}}\right)$	<p>Planar geometry.  <math>t &lt; 0: T(x) = T_\infty,</math>  <math>t &gt; 0: T(0) = T_0,</math>  <math>\dot{Q}(0,t) = kA \frac{T_0 - T_\infty}{\sqrt{\pi at}}</math></p>
<p>2. Step jump in surface heat flux</p> 	$\frac{T(x,t) - T_\infty}{\frac{\dot{Q}_0 x}{kA}} = \frac{\exp\left(\frac{-x^2}{4at}\right)}{\sqrt{\pi} \frac{x}{2\sqrt{at}}} - \operatorname{erfc}\left(\frac{x}{2\sqrt{at}}\right)$ $T(0,t) - T_\infty = \frac{\dot{Q}_0}{kA} \sqrt{\frac{4at}{\pi}}$	<p>Planar geometry.  <math>t &lt; 0: T(x) = T_\infty,</math>  <math>t &gt; 0: \frac{\dot{Q}_0}{A} = k \left. \frac{dT}{dx} \right _{x=0}</math></p>
<p>3. Step jump in surface convection</p> 	$\frac{T(x,t) - T_\infty}{T_0 - T_\infty} = \operatorname{erfc}\left(\frac{x}{2\sqrt{at}}\right) +$ $- \exp\left(\frac{hx}{k} + \frac{h^2 at}{k^2}\right) \operatorname{erfc}\left(\frac{x}{2\sqrt{at}} + \frac{h\sqrt{at}}{k}\right)$ $\frac{T(x,t) - T_\infty}{T_0 - T_\infty} \xrightarrow{t \rightarrow 0} \frac{h}{k} \sqrt{\frac{4at}{\pi}},$ $\frac{T(x,t) - T_\infty}{T_0 - T_\infty} \xrightarrow{t \rightarrow \infty} 1 - \frac{k}{h} \frac{1}{\sqrt{\pi at}}$	<p>Planar geometry.  <math>t &lt; 0: T(x) = T_\infty,</math>  <math>t &gt; 0:</math>  <math>\left. \frac{dT}{dx} \right _{x=0} = \frac{h}{k} (T_0 - T _{x=0})</math></p>
<p>4. Sudden thermal contact</p> 	$T(x \geq 0) = c_1 + c_2 \operatorname{erf}\left(\frac{x}{2\sqrt{a_A t}}\right)$ $T(x \leq 0) = c_3 + c_4 \operatorname{erf}\left(\frac{x}{2\sqrt{a_B t}}\right)$ $T_0 = \frac{T_A \sqrt{k_A \rho_A c_A} + T_B \sqrt{k_B \rho_B c_B}}{\sqrt{k_A \rho_A c_A} + \sqrt{k_B \rho_B c_B}}$	<p>Planar geometry.  <math>t &lt; 0: T(x) _{x&gt;0} = T_A</math> and <math>T(x) _{x&lt;0} = T_B.</math>  <math>t &gt; 0: T_0 \neq f(t).</math>          If equal properties:  <math>T_0 = (T_A + T_B) / 2</math></p>

## Freezing and thawing

Temperature variation due to heat transfer, may give way to a phase change, either in a pure-component medium (e.g. condensation of steam), or in a multi-component medium (e.g. condensation of water-vapour from humid air). In any case, when a phase change occurs, the associated enthalpy change must be accounted for, what, in addition to the density change involved, renders the problem difficult to model and solve. Conduction with phase change basically reduces to the classical Stefan problem, named after

Jožef Stefan, the Slovene physicist who introduced the general class of such problems around 1890, in relation to problems of ice formation.

Although an exact analytical formulation for this conduction moving-boundary problem [exists](#), the simpler following approximation is good enough in practice. Consider the one-dimensional freezing of a liquid of freezing temperature  $T_f$ , freezing enthalpy  $h_{SL}$ , density  $\rho$ , and thermal conductivity  $k$ , when exposed to a freezing medium (e.g. cold air) at a temperature  $T_\infty$  below its freezing point and with a convection coefficient  $h$ . After some time  $t$ , the freezing front will have progressed a distance  $X(t)$ , and a linear temperature profile may be assumed within the grown solid, from an unknown temperature  $T_0(t)$  at  $x=0$ , to the freezing front  $T_f$  at  $x=X$ . If the liquid is initially at  $T_f$ , then the energy balance per unit area at the freezing interface gives the growing rate:

$$\rho h_{SL} \frac{dX}{dt} = k \frac{T_f - T_0}{X} = h(T_0 - T_\infty) = \frac{T_f - T_\infty}{\frac{X}{k} + \frac{1}{h}} \Rightarrow X(t) = \frac{k}{h} \left( 1 - \sqrt{1 - \frac{2h^2(T_f - T_\infty)}{\rho h_{SL} k} t} \right) \quad (45)$$

The time  $\Delta t$  it takes to get a given frozen depth,  $X$ , is then:

$$\Delta t = \frac{\rho h_{SL}}{(T_f - T_\infty)} X \left( \frac{1}{h} + \frac{X}{2k} \right) \quad (46)$$

which can be generalised for other geometries by using the equivalent penetration depth defined as the quotient between volume and surface area,  $X=V/A$ ; i.e. for a slab of thickness  $L$ , one must set  $X=L/2$  in (46); for a cylinder of diameter  $D$ ,  $X=D/4$ ; and for a sphere,  $X=D/6$ .

The result (46) can also be applied to the freezing of a liquid flowing along a pipe at low Reynolds number (say at  $RePr < 10$ ). For instance, if a sizeable stretch of a capillary tube of internal radius  $R=1$  mm, through which water is flowing at 1 mm/s, is suddenly brought to a wall temperature 1 °C below freezing point, the time it will take for the flow to stop (when the growing ice reached the centre) is  $\Delta t = \rho h_{SL} X^2 / (2ks\Delta T) = \rho h_{SL} R^2 / (8ks\Delta T) = 1000 \cdot 334 \cdot 10^3 \cdot (10^{-3})^2 / (8 \cdot 2.3 \cdot 1) = 18$  s. At these low flow regimes, the ice/water interface is almost cylindrical (except near the entrance to the freezing segment), with the radius decreasing in time as  $r_{ice}/R = 1 - \sqrt{t/\Delta t}$ . For higher convection regimes, the closure time depends on flow speed, and the liquid may even go through the freezing stretch without becoming totally frozen.

## Reduction by separation of variables

There are problems described by partial differential equations whose initial and boundary conditions only depend on the variables alone and not on their combination. In those cases, looking for a solution in terms of functions of separate variables may transform the partial differential equation into a set of ordinary differential equations, one in each dimension, a technique developed by Fourier. Table 7 gives a compilation of analytical solutions to heat transfer problems in terms of separate variables.

Related to separation-of-variables method, some other approaches have been developed for the analytical and numerical solution of PDE problems, aiming at the reduction of one differentiation variable, the time variable in modal analysis (spectral methods), or one of the space variables in the integral-transform technique. For instance, for problems with restrictions varying with time, numerical methods become costly because one must always start at time  $t=0$  and use a small  $\Delta t$  for accuracy and stability. It is better to approximate the solution function in terms of eigenfunctions, obtained by solving the unloaded system  $(K-\lambda I)T_i=0$ , where  $\lambda_i$  are the eigenvalues and  $f_i = \frac{1}{2\pi} \sqrt{\lambda_i}$  the eigenfrequencies.

### Unsteady problems in 1-D

Some analytical solutions to unsteady problems have been developed above in terms of a similarity variable. Those apply basically to unbounded or semi-infinite media. When finite lengths (or finite times, as in periodic boundary conditions) appear in the problem, separation of variables can be tried, although, contrary to similarity solutions, separation of variables usually require an infinite series of terms to match the boundary conditions imposed, what reduces its practical interest.

Consider, for instance, thermal relaxation in a slab of thickness  $L$  and initial temperature  $T(x,0)$  when its surface temperature (on both sides) is maintained at a constant value  $T_0$ ; the particular case with  $T(0,t)=T_1$  serves to model the sudden immersion of a uniform-temperature solid into a stirred bath. The heat equation for this problem, assuming the solution  $T(x,t)$  can be cast in separate-variable functions, and after division by  $T(x,t)$ , becomes:

$$\frac{\partial^2 T}{\partial x^2} - \frac{1}{a} \frac{\partial T}{\partial t} = 0 \quad \xrightarrow{T(x,t)=F_1(x)F_2(t)} \quad \frac{d^2 F_1(x)}{F_1(x) dx^2} - \frac{1}{a} \frac{dF_2(t)}{F_2(t) dt} = 0 \quad (47)$$

showing that each term must be a constant (cannot depend on the other variable). The two kinds of functions that have a second derivative proportional to the function values are the exponential and trigonometric functions. We know that time-variation must be an exponentially-decaying function in all transient problems towards a stationary state, so that, because of the sign in (47), trigonometric functions must be chosen for the spatial dependence, whose actual form is dictated by the type of boundary conditions: if, as in our case, a constant value of the function must be maintained at the surface, the simplest choice is of the type  $X(x)=\sum c_n \sin(n\pi x/L)$  (maybe with an additional constant), which cancels at both  $x=0$  and  $x=L$ , or equivalently  $X(x)=\sum c_n \cos((n+1/2)\pi x/L)$ . In other cases, a zero temperature-gradient is imposed (adiabatic end), and thence the best choice is  $X(x)=\sum c_n \cos(n\pi x/L)$ , or equivalently  $X(x)=\sum c_n \sin((n+1/2)\pi x/L)$ . In our case, and with  $\Delta T \equiv T(x,t) - T_1$ , the solution is:

$$\Delta T(x,t) = \sum_{n=1}^{\infty} c_n \sin\left(\frac{n\pi x}{L}\right) \exp\left(-\frac{n^2 \pi^2 a t}{L^2}\right) \quad \text{with} \quad \begin{cases} \Delta T(x,0) = \sum_{n=1}^{\infty} c_n \sin\left(\frac{n\pi x}{L}\right) \\ \Delta T(0,t) = 0 \\ \Delta T(L,t) = 0 \end{cases} \quad (48)$$

Notice that the two boundary conditions  $\Delta T(0,t)=\Delta T(L,t)=0$  are automatically fulfilled by our choice of spatial base functions, whereas matching the generic initial boundary condition demands a Fourier-series expansion; the series coefficients are computed by minimisation of the function-projection over each of the base functions:

$$c_n = \frac{2}{L} \int_0^L \Delta T(x,0) \sin\left(\frac{n\pi x}{L}\right) dx, \quad n = 1, 2, 3 \dots \quad (49)$$

For instance, for a uniform initial temperature  $T_0$ ,  $\Delta T(x,0)=T_0-T_1$ , (49) yields  $c_n=(1-(-1)^n)2(T_0-T_1)/(n\pi)$ , and the evolution is as sketched in Fig. 5 using a truncated series,  $n=1..N$ .

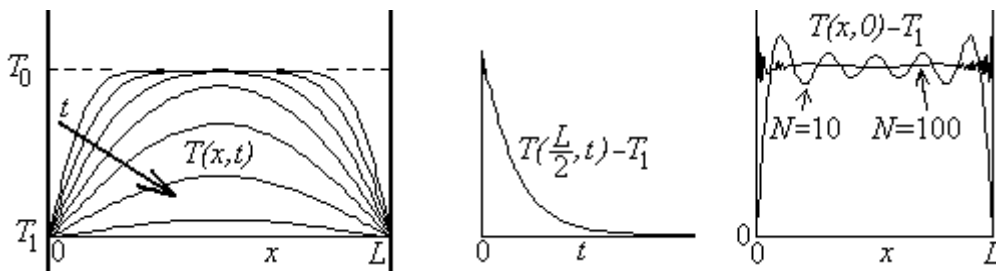


Fig. 5. Thermal relaxation in a slab of uniform initial temperature  $T_0$ , when suddenly brought to  $T_1$  at the ends: a) temperature profiles at several times, b) mid-point temperature evolution, and c) degree of matching the initial conditions for a truncated series with  $N=10$  and  $N=100$ ; notice that both approximations are nearly indistinguishable in a) and b).

The case of a planar geometry with one end suddenly brought to a higher temperature while the other is adiabatic, is presented in Fig. 6 and solved next.

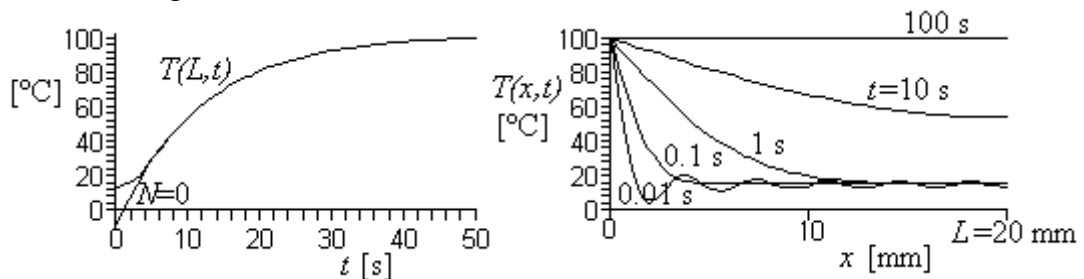


Fig. 6. Adiabatic wall with a temperature jump at one face. a) Rear temperature evolution approximated by just the first term in (50) ( $N=0$ , which gives  $T=53.5$  °C after 10 s, but is inappropriate below some 2 s), and a good-enough fit ( $N=10$ , which gives  $T=53.6$  °C after 10 s); b) temperature profiles along the plate using (49) truncated to  $N=10$  (notice that this approximation is inappropriate for times below 0.1 s).

**Exercise 9.** A 20 mm thick iron plate, initially at room temperature  $T_0=15$  °C, is suddenly brought to  $T_1=100$  °C on one face (e.g. by a jet of boiling water) while the other one can be considered isolated. Find the temperature at the rear 10 seconds after the change.

**Solution.** We try a solution to the heat equation in separate variables of the form:

$$T(x,t) = T(x,\infty) + \sum_{n=0}^{\infty} c_n \sin(a_n x) \exp(-b_n t) \text{ with } \begin{cases} T(x,0) = T(x,\infty) + \sum_{n=0}^{\infty} c_n \sin(a_n x) \\ \sin(a_n x)|_{x=0} = 0 \\ \left. \frac{d}{dx} \sin(a_n x) \right|_{x=L} = 0 \end{cases} \quad (50)$$

From the last condition (adiabatic rear:  $a_n \cos(a_n L) = 0$ ) one concludes that  $a_n L = \pi/2 + n\pi$ , and with (47),  $b_n = (n+1/2)^2 \pi^2 at/L^2$ ; thence:

$$T(x,t) = T_1 + \sum_{n=0}^{\infty} c_n \sin\left(\left(n + \frac{1}{2}\right)\pi \frac{x}{L}\right) \exp\left(-\left(n + \frac{1}{2}\right)^2 \frac{\pi^2 at}{L}\right)$$

$$\text{with } \sum_{n=0}^{\infty} c_n \sin\left(\left(n + \frac{1}{2}\right)\pi \frac{x}{L}\right) = T_0 - T_1 \Rightarrow c_n = \frac{2(T_0 - T_1)}{\left(n + \frac{1}{2}\right)\pi} \quad (51)$$

The rear temperature, plotted in Fig. 6 (as well as several spatial profiles), is then approximated by the truncated series (as seen in Fig. 6, the first term is already good enough for not too-short times):

$$\frac{T(L,t) - T_1}{(T_0 - T_1)} = \sum_{n=0}^N \frac{2(-1)^n}{\left(n + \frac{1}{2}\right)\pi} \exp\left(-\left(n + \frac{1}{2}\right)^2 \frac{\pi^2 at}{L^2}\right)$$

$$\approx \frac{4}{\pi} \exp\left(-\frac{\pi^2 at}{4L^2}\right) = \frac{4}{\pi} \exp\left(-\frac{\pi^2 13.7 \cdot 10^{-6} \cdot 10}{4 \cdot (0.02)^2}\right) = 0.547 \quad (52)$$

and finally  $T = 100 + (15 - 100) \cdot 0.547 = 53.5 \text{ }^\circ\text{C}$

There are many other standard separate-variable-solutions to one-dimensional unsteady problems, like those of non-trivial initial thermal fields, periodic boundary conditions, cylindrical or spherical geometries, etc., some of them compiled in Table 7. The case for the sudden immersion of slabs, cylinders, or spheres, in a fluid is of so much practical interest that graphical presentations are commonly used (following the first plots by M.P.Heisler-1947); these so-called Heisler's diagrams, present the non-dimensional temperature and non-dimensional heat-flux in terms of the only two non-dimensional parameters involved: the non-dimensional time given by the Fourier number,  $Fo \equiv at/R^2$ , and the non-dimensional heat-convection coefficient expressed by the Biot number,  $Bi \equiv hR/k$ . Nowadays, with the availability of computers, the usefulness of these kind of graphical presentations has declined.

The case of a spherical geometry is presented in Fig. 7 and solved next.

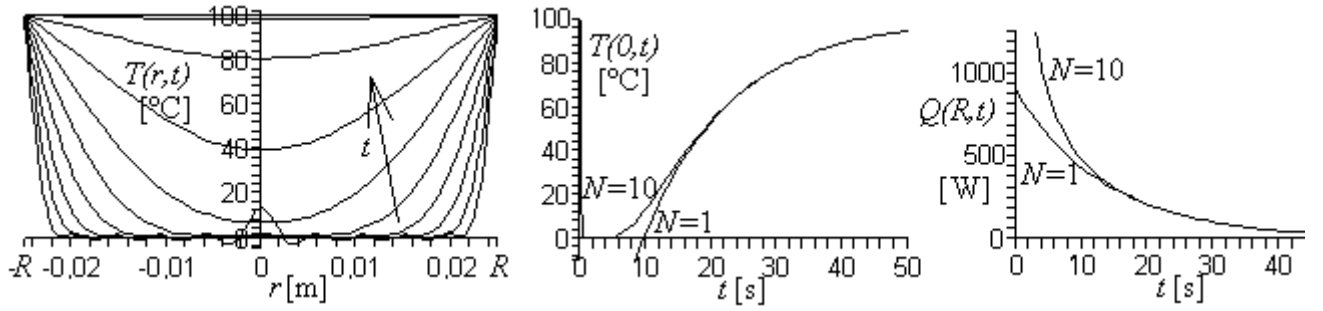


Fig. 7. Temperature and heat-flow evolution in a sphere at 0 °C suddenly exposed to 100 °C.

**Exercise 10.** Find the central temperature evolution in a stainless-steel ball 5 cm in diameter, when taken out of an ice-water bath and submerged into boiling water.

**Solution.** Instead of just using the solution given in Table 8, we develop here the result from the basic heat equation (and with two different boundary conditions):

$$\frac{1}{a} \frac{\partial T}{\partial t} = \frac{1}{r^2} \frac{\partial}{\partial r} \left( r^2 \frac{\partial T}{\partial r} \right) \xrightarrow{T(r,t)=F_1(r)F_2(t)} \frac{1}{a} \frac{dF_2(t)}{F_2(t)dt} = \frac{2}{r} \frac{dF_1(r)}{F_1(r)dr} + \frac{d^2 F_1(r)}{F_1(r)dr^2} \quad (53)$$

showing that each term must be a constant (cannot depend on the other variable). We know that time-variation must be an exponentially-decaying function in all transient problems towards a stationary state, so that the mentioned constant must be negative, say  $-b^2$ . The solution to the left-hand-side,  $dF_2(t)/dt = -b^2 a$ , is then  $F_2(t) = c_1 \exp(-b^2 a t)$ , whereas the solution to the right-hand-side, with the change  $G(r) = F_1(r)/r$ , becomes,  $d^2 G(r)/dr^2 = -b^2$ , and thus has as solutions  $F_1(r) = c_2 \sin(br)/r + c_3 \cos(br)/r$ , although only the sin-term is appropriate here since  $F_1(r)|_{r=0}$  must be finite. The general solution to (53) is then:

$$T(r,t) = T(r,\infty) + \sum_{n=1}^{\infty} c_n \frac{\sin(b_n r)}{r} \exp(-b_n^2 a t) \quad (54)$$

where the constants  $c_n$  and  $b_n$  are obtained by imposing initial and boundary conditions.

If we model the convective boiling process by the limit  $h \rightarrow \infty$ , then the initial and boundary conditions are:

$$T(r,0) = T_0 = T_1 + \sum_{n=1}^{\infty} c_n \frac{\sin(b_n r)}{r} \quad (55)$$

$$\left. \frac{dT(r,t)}{dr} \right|_{r=0} = 0 \quad (56)$$

$$T(R,t) = T_1 + \sum_{n=1}^{\infty} c_n \frac{\sin(b_n R)}{R} \exp(-b_n^2 a t) \quad (57)$$

From (57) we deduce that  $b_n R = n\pi$ , (56) is automatically verified, and from (55), with the value for  $b_n$ , we get  $c_n = -2(-1)^n (T_1 - T_0) / (n\pi)$ , finally yielding:



$$\frac{T(r,t)-T_1}{T_0-T_1} = \sum_{n=1}^{N \rightarrow \infty} \frac{2(-1)^n \sin\left(\frac{n\pi r}{R}\right)}{\frac{n\pi r}{R}} \exp(-n^2\pi^2 at) \quad (58)$$

with the results presented in Fig. 7 for  $N=10$  and the data for this exercise:  $T_0=0$  °C for the ice bath,  $T_1=100$  °C for the boiling bath,  $R=0.025$  m, and  $a=k/(\rho c)=18/(7800 \cdot 500)=4.6 \cdot 10^{-6}$  m<sup>2</sup>/s for stainless-steel. We may check the order of magnitude of the relaxation time,  $\Delta t=L^2/a=(0.05/6)^2/4.6 \cdot 10^{-6}=15$  s (to be compared with the real relaxation time of some 30 s estimated from Fig. 7), where the characteristic length of a spherical object,  $L=V/A=(\pi D^3/6)/(\pi D^2)=D/6$ , has been used.

If we model the convective boiling process by a finite-value convective coefficient,  $h$ , then the initial and boundary conditions to be imposed on (54) are:

$$T(r,0) = T_0 = T_1 + \sum_{n=1}^{\infty} c_n \frac{\sin(b_n r)}{r} \quad (59)$$

$$\left. \frac{dT(r,t)}{dr} \right|_{r=0} = 0 \quad (60)$$

$$\left. -k \frac{dT(r,t)}{dr} \right|_{r=R} = h(T(R,t) - T_1) \quad (61)$$

Developing (57) we get:

$$\begin{aligned} -k \sum_{n=1}^{\infty} c_n \left[ \frac{b_n \cos(b_n R)}{R} - \frac{\sin(b_n R)}{R^2} \right] \exp(-b_n^2 at) &= h \sum_{n=1}^{\infty} c_n \frac{\sin(b_n R)}{R} \exp(-b_n^2 at) \\ -\frac{b_n R \cos(b_n R)}{\sin(b_n R)} + 1 &= \frac{hR}{k} \equiv Bi \end{aligned} \quad (62)$$

and we cannot proceed any further analytically since the values for  $b_n$  must be obtained by numerically solving (62). Once this is done, values for  $c_n$  are obtained by cancelling the projection of (59) over each of its base-functions, with the final result shown in Fig. 8. Now, both the temperature at the centre and the temperature at the surface are shown versus time; notice that this relaxation process is slower than the former: e.g. after 30 s, the centre-temperature is now 61 °C, the heat flow is 240 W, and 82% of the energy transfer has occurred, whereas in the constant-surface-temperature model, after 30 s, the centre-temperature is 78 °C and the energy received 93% of the total.

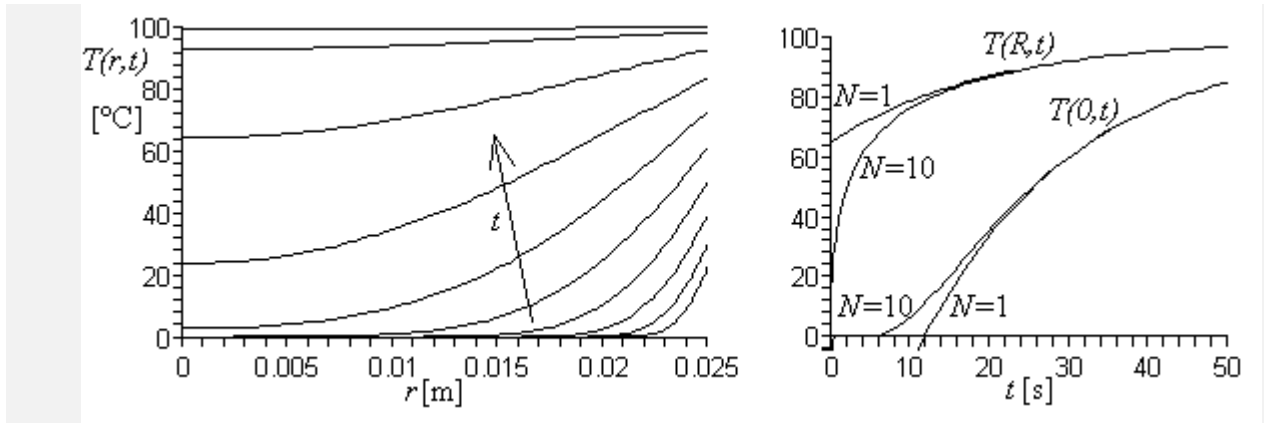


Fig. 8. Temperature and heat-flow evolution in a sphere brought from 0 °C to 100 °C, (58).

### Periodic solutions in 1-D

For problems with periodic boundary conditions, a more involved separation of variables must be applied, and only suitable when the periodic response has been achieved, after the initial transients following the periodic excitation. For a semi-infinite solid with periodic boundary conditions, the physical variables  $(x,t)$  are changed to the new variables  $(x/x_c, 2\pi t/\tau - x/x_c)$ , corresponding to a time-shift proportional to penetration distance, and dependent on the applied period  $\tau$  and a characteristic length  $x_c$  (to be found from the heat equation), as shown in the following Exercise.

**Exercise 11.** Find the penetration of the thermal wave when a sinusoidal temperature-variation is forced in the surface of a semi-infinite solid.

**Solution.** We try a solution to the heat equation that is periodic in time, with the applied period  $\tau$ , and decays exponentially with a characteristic penetration length  $x_c$  to be found:

$$\frac{\partial^2 T}{\partial x^2} - \frac{1}{a} \frac{\partial T}{\partial t} = 0 \quad \xrightarrow{T(x,t) = C \exp(-x/x_c) \cos(2\pi t/\tau - x/x_c)} \quad 2C \frac{a\tau - \pi x_c^2}{a\tau x_c^2} \exp\left(-\frac{x}{x_c}\right) \sin\left(\frac{2\pi t}{\tau} - \frac{x}{x_c}\right) = 0$$

$$\Rightarrow x_c = \sqrt{\frac{a\tau}{\pi}} \quad \rightarrow \quad \frac{T(x,t) - T_{0,\text{mean}}}{T_{0,\text{max}} - T_{0,\text{mean}}} = \exp\left(-\frac{x}{x_c}\right) \cos\left(\frac{2\pi t}{\tau} - \frac{x}{x_c}\right) \quad (63)$$

i.e., the  $T$ -oscillation amplitude imposed on the surface, decays with penetration, being a fraction  $\exp(-1)=0.37$  at  $x=x_c$ , a fraction  $\exp(-2)=0.13$  at  $x=2x_c$ , a fraction  $\exp(-3)=0.05$  at  $x=3x_c$ , and so on, with the result that for  $x \gg x_c$  the oscillations are unnoticeable, and such a finite-thickness wall can be considered semi-infinite in this respect. But the most interesting result is the time-lag between the maximum  $\Delta T$  at  $x=x_c$  relative to the maximum  $\Delta T$  at  $x=0$ ; as said,  $\Delta T_{x_c}/\Delta T_0=0.37$ , and it occurs after a time-lag of  $\tau/(2\pi)$ , i.e. around a sixth of the period later; for instance, if the model is applied to the annual temperature oscillations in temperate climates,  $\tau=1$  yr and the maximum temperature at a depth of  $x=x_c=(a\tau/\pi)^{1/2}=(10^{-6} \cdot 31.5 \cdot 10^6/\pi)^{1/2}=3$  m is retarded  $\tau/(2\pi)=2$  months relative to the maximum at the surface (say, the summer solstice), where a typical thermal diffusivity for the land  $a=10^{-6}$  m<sup>2</sup>/s, and the approximation of imposed variation of surface temperature, have been assumed. Similarly, the diurnal temperature change at a depth of  $x_c=(a\tau/\pi)^{1/2}=(10^{-6} \cdot 86400/\pi)^{1/2}=0.17$  m below ground is dumped to 37% of the surface amplitude,

and delayed about  $\tau/(2\pi)=4$  h relative to the maximum at the surface (midday). These results can be applied to the finding of a minimum depth to bury water pipes to avoid freezing in cold weather; e.g. in a given location with diurnal extreme temperatures of  $-6$  °C and  $+14$  °C, i.e.  $T=(4\pm 10)$  °C, placing the pipes  $x_c=0.17$  m below the surface already shortens the oscillations to  $T=(4\pm 10 \cdot \exp(-1))$  °C  $= (4\pm 3.7)$  °C, thus avoiding freezing.

The thermal penetration depth is very small for metals exposed to rapid temperature oscillations, as for piston-cylinder walls in reciprocating engines; e.g. for a two-stroke 6000 rpm operation,  $\tau=0.01$  s, and with a metal thermal diffusivity of  $a=10^{-4}$  m<sup>2</sup>/s, the semi-infinite heat-transfer model can be applied to wall thicknesses larger than  $x=x_c=(a\tau/\pi)^{1/2}=(10^{-4} \cdot 10^{-2}/\pi)^{1/2}=0.6$  mm.

The heat flux corresponding to solution (63),  $\dot{q} = -k\nabla T$ , also shows a periodic oscillation in time and a decreasing amplitude with depth. In particular, the heat flow at the surface is:

$$\dot{q}(0,t) = k\sqrt{\frac{2\pi}{a\tau}} \cos\left(\frac{2\pi t}{\tau} - \frac{\pi}{4}\right) \quad \text{due to} \quad T_0(t) = T_{0,\text{mean}} + (T_{0,\text{max}} - T_{0,\text{mean}}) \cos\left(\frac{2\pi t}{\tau}\right) \quad (64)$$

### Example 2. Temperature oscillations in an engine wall

Related to this planar oscillatory solution is the spherical solution, i.e. where a point heat source at the origin ( $r=0$ ) has a periodic amplitude,  $\dot{Q}_0 = \dot{Q}_{0m} \sin(2\pi t/\tau)$ . The temperature field (singular at  $r=0$ ) is:

$$T(r,t) = \frac{\dot{Q}_{0m}}{4\pi k r} \exp\left(-\frac{r}{r_c}\right) \sin\left(\frac{2\pi t}{\tau} - \frac{r}{r_c}\right) \quad \text{with} \quad r_c = \sqrt{\frac{a\tau}{\pi}} \quad (65)$$

### **Steady problems in 2-D**

The separation-of-variables technique can be applied to higher order multi-dimensional problems (as before, initial and boundary conditions must be also stated in separated variables).

In the general case of unsteady problems, the solution can be built by combination of the one-dimensional problems involved. For instance, the temperature field in a finite cylinder of length  $L$  and radius  $R$ , initially at  $T_0$ , when subjected to lateral convection with coefficient  $h_1$  and fluid temperature  $T_1$ , to some other constant convective coefficient  $h_2$  at the upper base, with the far fluid at temperature  $T_2$ , is  $T(r,z,t)=T_{\text{cyl}}(r,t)T_{\text{slab}}(x,t)$ , where  $T_{\text{cyl}}(r,t)$  is the solution given in Table 7 (case 11) for the infinite cylinder exposed to lateral convection, and  $T_{\text{slab}}(x,t)$  is the solution given in Table 7 (case 5) for the slab with a convective condition at  $x=L$  and an adiabatic condition at  $x=0$ . In summary:

$$T(x,y,z,t) = T_{\text{caseA}}(x,t)T_{\text{caseB}}(y,t)T_{\text{caseC}}(z,t) \quad (66)$$

It can be demonstrated that the heat transfer can also be computed by composition of the one-dimensional cases, in the way (Langston-1982):

$$\frac{\dot{Q}(x, y, z, t)}{\dot{Q}_0} = \frac{\dot{Q}_{caseA}}{\dot{Q}_0} + \frac{\dot{Q}_{caseB}}{\dot{Q}_0} \left(1 - \frac{\dot{Q}_{caseA}}{\dot{Q}_0}\right) + \frac{\dot{Q}_{caseC}}{\dot{Q}_0} \left(1 - \frac{\dot{Q}_{caseB}}{\dot{Q}_0}\right) \left(1 - \frac{\dot{Q}_{caseA}}{\dot{Q}_0}\right) \quad (67)$$

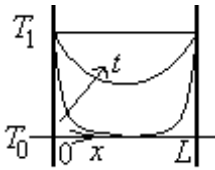
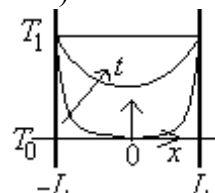
For steady problems, the unsteady solutions constructed as said before can be applied in the limit  $t \rightarrow \infty$ , or new solutions in separate variables built from scratch. For instance, if we consider a two-dimensional slab of widths  $L_x$  and  $L_y$ , initially at  $T_0$ , with one of its sides, say  $y=L_y$ , brought to  $T_1$  (the other three sides are kept at  $T_1$ ), the formulation is as follows:

$$\begin{aligned} \frac{\partial^2 T(x, y)}{\partial x^2} + \frac{\partial^2 T(x, y)}{\partial y^2} = 0 &\xrightarrow{T(x, y) = X(x)Y(y)} \frac{\partial^2 X(x)}{X(x) \partial x^2} + \frac{\partial^2 Y(y)}{Y(y) \partial y^2} = 0 \\ \text{with } \begin{cases} X(0) = T_0, X(L_x) = T_0 \\ Y(0) = T_0, Y(L_y) = T_1 \end{cases} &\Rightarrow \begin{cases} X(x) = c_n \sin\left(\frac{n\pi x}{L_x}\right) \\ Y(y) = \sinh\left(\frac{n\pi y}{L_y}\right) \end{cases} \Rightarrow \\ \rightarrow \frac{T - T_0}{T_1 - T_0} = \frac{2}{\pi} \sum_{n=1}^{\infty} \frac{1 - (-1)^n}{n \sinh(n\pi L_y / L_x)} \sin\left(\frac{n\pi x}{L_x}\right) \sinh\left(\frac{n\pi y}{L_x}\right) &\quad (68) \end{aligned}$$

where the trigonometric functions have been selected in  $X(x)$  because of the periodicity in the  $x$ -boundary-conditions, whereas the hyperbolic functions are chosen for  $Y(y)$  because of the exponential adaptation from  $T_0$  to  $T_1$ .

As a final remark, all these analytical solutions in series-expansions should be considered mainly as interesting academic solutions, but of very limited practical use, because a simple finite-difference numerical simulation resolves all these regular-boundary problems with a single code and similar programming burden, and practical non-rectangular geometries have to be solved numerically anyway.

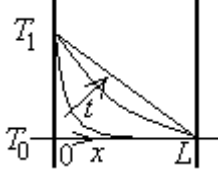
Table 7. Some analytical solutions for the heat equation in terms of separate variables ( $\Delta T \equiv T(x, t) - T_{ini}$ ).

Problem	Solution
1. Slab. $T$ -jump on both sides. 	$0 < x < L, T(x, 0) = T_0, T(x, \infty) = T_1:$ $\frac{T(x, t) - T_1}{T_0 - T_1} = \frac{2}{\pi} \sum_{n=1}^{\infty} \frac{1 - (-1)^n}{n} \sin\left(\frac{n\pi x}{L}\right) \exp\left(-\frac{n^2 \pi^2 at}{L^2}\right)$ $\dot{q}(0, t) = \frac{2k(T_0 - T_1)}{L} \sum_{n=1}^{\infty} (1 - (-1)^n) \exp\left(-\frac{n^2 \pi^2 at}{L^2}\right)$
2. Slab. $T$ -jump on both sides (centred). 	$-L < x < L, T(x, 0) = T_0, T(x, \infty) = T_1:$ $\frac{T(x, t) - T_1}{T_0 - T_1} = \frac{2}{\pi} \sum_{n=1}^{\infty} \frac{1 - (-1)^n}{n} \sin\left(\frac{n\pi(x+L)}{2L}\right) \exp\left(-\frac{n^2 \pi^2 at}{4L^2}\right)$ $\dot{q}(L, t) = \frac{k(T_0 - T_1)}{L} \sum_{n=1}^{\infty} (1 - (-1)^n) \exp\left(-\frac{n^2 \pi^2 at}{4L^2}\right)$ or else

$$\frac{T(x,t)-T_0}{T_1-T_0} = \frac{4}{\pi} \sum_{n=0}^{\infty} \frac{(-1)^n}{2n+1} \cos\left(\frac{(2n+1)\pi x}{2L}\right) \exp\left(-\frac{(2n+1)^2 \pi^2 at}{4L^2}\right)$$

$$\dot{q}(L,t) = \frac{2k(T_0-T_1)}{L} \sum_{n=0}^{\infty} \exp\left(-\frac{(2n+1)^2 \pi^2 at}{4L^2}\right)$$

3. Slab.  $T$ -jump on one side.

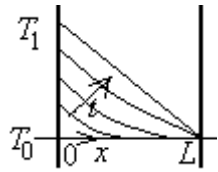


$0 < x < L$ ,  $T(x,0)=T_0$ ,  $T(x,\infty)=T_1-(T_1-T_0)x/L$ :

$$\frac{T(x,t)-T_1}{T_0-T_1} = \frac{x}{L} + \frac{2}{\pi} \sum_{n=1}^{\infty} \frac{1}{n} \sin\left(\frac{n\pi x}{L}\right) \exp\left(-\frac{n^2 \pi^2 at}{L^2}\right)$$

$$\dot{q}(0,t) = \frac{k(T_0-T_1)}{L} \left(1 - 2 \sum_{n=1}^{\infty} \exp\left(-\frac{n^2 \pi^2 at}{L^2}\right)\right)$$

4. Slab.  $\dot{Q}$ -jump on one side, and  $T=T_0$  at  $x=L$ .

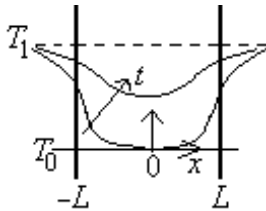


$0 < x < L$ ,  $T(x,0)=T_0$ ,  $T(x,\infty)=T_1-(T_1-T_0)x/L$ :

$$\frac{T(x,t)-T_0}{\frac{\dot{Q}_0}{kL}} = 1 - \frac{x}{L} + \frac{8}{\pi} \sum_{n=0}^{\infty} \frac{(-1)^n}{(2n+1)^2} \sin\left(\frac{(2n+1)\pi(L-x)}{2L}\right) \cdot \exp\left(-\frac{(2n+1)^2 \pi^2 at}{4L^2}\right)$$

$$\frac{\dot{Q}_L(0,t)}{\dot{Q}_0} = 1 - \frac{4}{\pi} \sum_{n=0}^{\infty} \frac{(-1)^n}{(2n+1)^2} \exp\left(-\frac{(2n+1)^2 \pi^2 at}{4L^2}\right)$$

5. Slab. Immersion in a fluid with constant- $h$ .



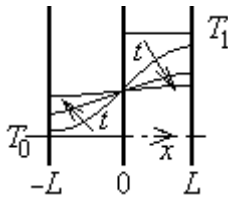
$-L < x < L$ ,  $T(x,0)=T_0$ ,  $T(x,\infty)=T_1$ :

$$\frac{T(x,t)-T_0}{T_{1,\infty}-T_0} = \sum_{n=1}^{\infty} \frac{4 \sin(c_n L)}{2c_n L + \sin(2c_n L)} \cos(c_n x) \exp(-c_n^2 at)$$

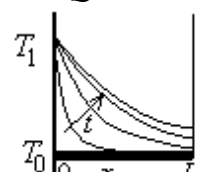
$$\frac{\dot{q}(L,t)L}{k(T_{1,\infty}-T_0)} = \sum_{n=1}^{\infty} \frac{4c_n L \sin^2(c_n L)}{2c_n L + \sin(2c_n L)} \exp(-c_n^2 at)$$

$c_n$  being the  $n$ -root of  $c_n L \tan(c_n L) = Bi \equiv \frac{hL}{k}$

6. Two slabs contacting with adiabatic ends.



7. Rod.  $T$ -jump on one side, and  $\dot{Q}=0$  at  $x=L$ .

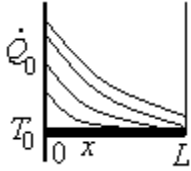


$0 < x < L$ ,  $T(x,0)=T_0$ ,  $T(x,\infty)=T_0+(Q_0)\cosh((m(L-x))/\cosh(mL))$ :

$$\frac{T(x,t)-T_0}{T_1-T_0} = \frac{\cosh[m(L-x)]}{\cosh(mL)} + \frac{4}{\pi} \sum_{n=0}^{\infty} \frac{2n+1}{(2n+1)^2 + 4m^2 L^2 / \pi^2} \cdot \sin\left(\frac{(2n+1)\pi x}{2L}\right) \exp\left(-\frac{(\pi^2 (2n+1)^2 + m^2 L^2) at}{4L^2}\right)$$

$$\frac{\dot{Q}(0,t)}{mkA(T_1-T_0)} = \tanh(mL) + \frac{2}{mL} \sum_{n=0}^{\infty} \frac{(2n+1)^2}{(2n+1)^2 + 4m^2L^2/\pi^2} \cdot \exp\left(-\frac{(\pi^2(2n+1)^2 + m^2L^2)at}{4L^2}\right)$$

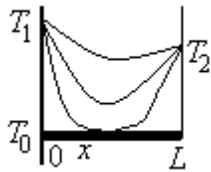
8. Rod.  $\dot{Q}$ -jump on one side, and  $\dot{Q}=0$  at  $x=L$ .



$0 < x < L$ ,  $T(x,0)=T_0$ ,  $T(x,\infty)=T_0 + (\dot{Q}_0/(mkA)) \cosh[m(L-x)]/\sinh(mL)$ :

$$\frac{T(x,t)-T_0}{\frac{\dot{Q}_0}{mkA}} = \frac{\cosh[m(L-x)]}{\sinh(mL)} \frac{\exp(-m^2at)}{mL} + 2mL \sum_{n=1}^{\infty} \frac{-1}{\pi^2n^2 + m^2L^2} \cos\left(\frac{n\pi x}{L}\right) \exp\left(-\frac{(\pi^2n^2 + m^2L^2)at}{L^2}\right)$$

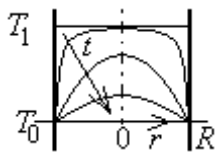
9. Rod.  $T$ -jump on both sides.



$0 < x < L$ ,  $T(x,0)=T_0$ ,  $T(x,\infty)=T_0 + (T_1-T_0)\sinh((m(L-x))/\sinh(mL) + (T_2-T_0)\sinh((mx)/\sinh(mL))$ :

$$T(x,t)-T_0 = (T_1-T_0) \frac{\sinh[m(L-x)]}{\sinh(mL)} + (T_2-T_0) \frac{\sinh(mx)}{\sinh(mL)} + \frac{2}{\pi} \sum_{n=0}^{\infty} \frac{n((T_1-T_0) - (-1)^n(T_2-T_0))}{(n^2 + m^2L^2/\pi^2)} \sin\left(\frac{n\pi x}{L}\right) \exp\left(-\frac{(\pi^2n^2 + m^2L^2)at}{L^2}\right)$$

10. Cylinder.  $T$ -jump at the surface.



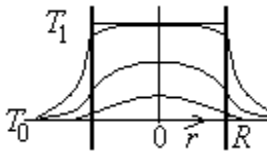
$0 < r < R$ ,  $T(r,0)=T_1$ ,  $T(r,\infty)=T_0$ :

$$\frac{T(r,t)-T_0}{T_1-T_0} = \sum_{n=1}^{\infty} \frac{2J_1(c_n R)}{c_n R (J_0^2(c_n R) + J_1^2(c_n R))} J_0(c_n r) \exp(-c_n^2 at)$$

$$\frac{\dot{q}(R,t)R}{k(T_1-T_0)} = \sum_{n=1}^{\infty} \frac{2J_0^2(c_n R)}{J_0^2(c_n R) + J_1^2(c_n R)} \exp(-c_n^2 at)$$

$c_n$  being the  $n$ -root of  $J_0(c_n R) = 0$

11. Cylinder. Immersion in a fluid with constant- $h$ .



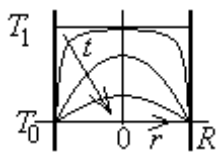
$0 < r < R$ ,  $T(r,0)=T_1$ ,  $T(r,\infty)=T_0$ :

$$\frac{T(r,t)-T_0}{T_{1,\infty}-T_0} = \sum_{n=1}^{\infty} \frac{2J_1(c_n R)}{c_n R (J_0^2(c_n R) + J_1^2(c_n R))} J_0(c_n r) \exp(-c_n^2 at)$$

$$\frac{\dot{q}(R,t)R}{k(T_{1,\infty}-T_0)} = \sum_{n=1}^{\infty} \frac{2J_0^2(c_n R)}{J_0^2(c_n R) + J_1^2(c_n R)} \exp(-c_n^2 at)$$

$c_n$  being the  $n$ -root of  $\frac{c_n R J_1(c_n R)}{J_0(c_n R)} = Bi \equiv \frac{hR}{k}$

12. Sphere.  $T$ -jump at the surface.



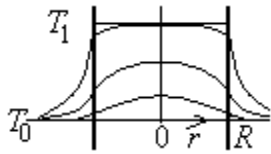
$0 < r < R$ ,  $T(r,0)=T_1$ ,  $T(r,\infty)=T_0$ :

$$\frac{T(r,t)-T_0}{T_1-T_0} = -2 \sum_{n=1}^{\infty} \frac{(-1)^n \sin\left(\frac{n\pi r}{R}\right)}{n \frac{n\pi r}{R}} \exp\left(-\frac{n^2 \pi^2 at}{R^2}\right)$$

$$\frac{\dot{q}(R,t)R}{k(T_1-T_0)} = 2 \sum_{n=1}^{\infty} \exp\left(-\frac{n^2 \pi^2 at}{R^2}\right)$$

13. Sphere. Immersion in a fluid with constant- $h$ .

$0 < r < R$ ,  $T(r,0)=T_1$ ,  $T(x,\infty)=T_0$ :



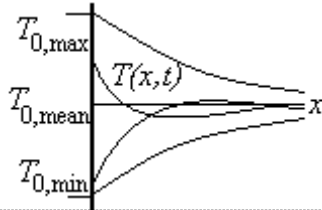
$$\frac{T(r,t) - T_0}{T_{1,\infty} - T_0} = \sum_{n=0}^{\infty} \frac{2(\sin(c_n R) - c_n R \cos(c_n R))}{c_n R (c_n R - \sin(c_n R) \cos(c_n R))} \frac{\sin(c_n r)}{r} \exp(-c_n^2 a t)$$

$$\frac{\dot{q}(R,t) R}{k(T_{1,\infty} - T_0)} = \sum_{n=0}^{\infty} \frac{2(c_n R \cos(c_n R) - \sin(c_n R))^2}{c_n R (c_n R - \sin(c_n R) \cos(c_n R))} \exp(-c_n^2 a t)$$

$$c_n \text{ being the } n\text{-root of } 1 - \frac{c_n R \cos(c_n R)}{\sin(c_n R)} = Bi \equiv \frac{hR}{k}$$

14. Semi-infinite body with periodic surface temperature.

$x > 0$ ,  $T(x,0) = T_{0,\text{mean}}$ ,  $T(0,t) = T_{0,\text{mean}} + \Delta T_0 \sin(2\pi t / \tau)$ ,  $\tau$  being the imposed period.

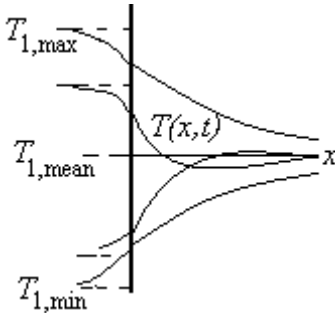


$$\frac{T(x,t) - T_{0,\text{mean}}}{T_{0,\text{max}} - T_{0,\text{mean}}} \stackrel{t \gg \tau}{=} \exp\left(-\frac{x}{x_c}\right) \sin\left(\frac{2\pi t}{\tau} - \frac{x}{x_c}\right), x_c \equiv \sqrt{\frac{a\tau}{\pi}}, a \equiv \frac{k}{\rho c}$$

$$\frac{\dot{q}(0,t)}{\sqrt{2k}(T_{0,\text{max}} - T_{0,\text{mean}})} = \sin\left(\frac{2\pi t}{\tau} + \frac{\pi}{4}\right)$$

15. Semi-infinite body with periodic surface convection.

$x > 0$ ,  $T(x,0) = T_{1,\text{mean}}$ ,  $T(-\infty,t) = T_{1,\text{mean}} + \Delta T_1 \sin(2\pi t / \tau)$

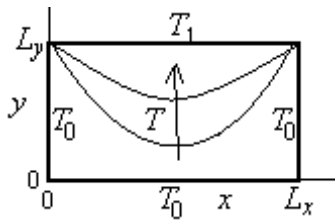


$$\frac{T(x,t) - T_{1,\text{mean}}}{T_{1,\text{max}} - T_{1,\text{mean}}} \stackrel{t \gg \tau}{=} \frac{1}{\sqrt{1 + \frac{2}{Bi} + \frac{2}{Bi^2}}} \exp\left(-\frac{x}{x_c}\right) \sin\left(\frac{2\pi t}{\tau} - \frac{x}{x_c} - \arctan\left(\frac{1}{1 + Bi}\right)\right)$$

$$Bi \equiv \frac{hx_c}{k}$$

$$\frac{\dot{q}(0,t)}{\sqrt{2k}(T_{1,\text{max}} - T_{1,\text{mean}})} = \frac{1}{\sqrt{1 + \frac{2}{Bi} + \frac{2}{Bi^2}}} \sin\left(\frac{2\pi t}{\tau} + \frac{\pi}{4} - \arctan\left(\frac{1}{1 + Bi}\right)\right)$$

16. Bi-dimensional steady state after a temperature-jump from  $T_0$  to  $T_1$  in part of its surface.



$T$ -jump only at the upper side (as in the sketch):

$$\frac{T(x,y) - T_0}{T_1 - T_0} = \frac{2}{\pi} \sum_{n=1}^{\infty} \frac{1 - (-1)^n}{n} \frac{\sinh\left(\frac{n\pi y}{L_x}\right) \sin\left(\frac{n\pi x}{L_x}\right)}{\sinh\left(\frac{n\pi L_y}{L_x}\right)}$$

$T$ -jump at the upper and right side (not in the sketch):

$$\frac{T(x,y) - T_0}{T_1 - T_0} = \frac{2}{\pi} \sum_{n=1}^{\infty} \frac{1 - (-1)^n}{n} \left[ \frac{\sinh\left(\frac{n\pi y}{L_x}\right) \sin\left(\frac{n\pi x}{L_x}\right)}{\sinh\left(\frac{n\pi L_y}{L_x}\right)} + \frac{\sinh\left(\frac{n\pi x}{L_y}\right) \sin\left(\frac{n\pi y}{L_y}\right)}{\sinh\left(\frac{n\pi L_x}{L_y}\right)} \right]$$

## Other analytical methods to solve partial differential equations

There are other well-known analytical methods used to solve partial differential equations, but their application in heat transfer is marginal. Among them we have:

- Green function integrals. For a given field (like the electrostatic field), Green's function gives the potential at the point  $x$  due to a point charge at the point  $x'$  the source point, and only depends on the

distance between the source and field points. For instance, for the two dimensional Laplace operator, Green's function is  $G(x,x')=-\ln r/(2\pi)$ , with  $r$  being the distance such that  $r^2=(x-x')^2+(y-y')^2$ , and a general solution to  $T_{xx}+T_{yy}-\phi(x,y)=0$  is  $T(x,y)= \iint G(x,x',y,y')\phi(x',y')dx'dy'$ . Green's functions play an important role in the solution of linear ordinary and partial differential equations, and are a key component to the development of boundary integral equation methods.

- Laplace transform. Laplace transform is a kind of Fourier integral that converts differential equations in time into algebraic equations, what renders it worth to convert time-dependant heat transfer problems to time-independent problems (but the reverse, finding the Laplace inverse function is not an easy task).

A final comment on analytical solutions is appropriate here. Although the superposition principle for linear differential equations allows for problems with complex boundary or initial conditions to be solved by series expansion or Green's function integrals, they would require numerical evaluation for the sums or integrals, and straight numerical methods are preferred

### Duhamel's theorem

Duhamel's theorem demonstrates that the solution to a (linear) heat conduction problem with time-dependent boundary conditions or/and time-dependent heat-sources,

$$\nabla^2 T(\bar{x},t) + \frac{\phi(\bar{x},t)}{k} - \frac{1}{a} \frac{\partial T(\bar{x},t)}{\partial t} = 0, \quad -k \frac{\partial T(\bar{x},t)}{\partial x_i} + hT(\bar{x},t) = f(t) \quad (69)$$

can be computed from the solution to a the time-independent problem:

$$\nabla^2 T(\bar{x},t,\tau) + \frac{\phi(\bar{x},\tau)}{k} - \frac{1}{a} \frac{\partial T(\bar{x},t,\tau)}{\partial t} = 0, \quad -k \frac{\partial T(\bar{x},t,\tau)}{\partial x_i} + hT(\bar{x},t,\tau) = f(\tau) \quad (70)$$

where  $t$  is now a parameter (not time), with the relation:

$$T(\bar{x},t) = \frac{\partial}{\partial t} \int_{\tau=0}^{\tau=t} T(\bar{x},t-\tau,\tau) d\tau \quad (71)$$

## NUMERICAL SOLUTIONS

Numerical solutions are the rule in solving practical heat transfer problems, as well as in mass and momentum transfer, because the analytical formulation in terms of partial differential equations is not analytically solvable except for very simple configurations, as seen above. Numerical methods transform the continuous problem to a discrete problem, thus, instead of yielding a continuous solution valid at every point in the system and every instant in time, and every value of the parameters, numerical methods only yield discrete solutions, valid only at discrete points in the system, at discrete time intervals, and for discrete values of the parameters. However gloom the numerical approach may sound, it has two crucial advantages:

- Can provide a solution to any practical problem, however complicated it may be (not just steady one-dimensional, constant-property ideal models). In any case, it is most important to realise that



any practical problem is at the end an intermediate idealisation aiming at practical answers (e.g. nobody takes account of the infinite figures in  $\pi$ , 3 may be a good-enough approximation, and 3.1416 already an accuracy illusion).

- The discretization can be refined as much as wanted (of course, at the expense in computing time and memory, and operator's burden). In any case, it is wise to start with as few unknowns as feasible, for an efficient feedback (most of the first trials suffer from infancy problems that are independent on the finesse of the discretisation). Any good practitioner knows that refinements should follow coarse work, and not the contrary.

All numerical approaches transform the continuous problem, that we may write as  $PDE(T)=F$  meaning that a partial differential operator applied to the temperature field should equal the force-field imposing the thermal non-equilibrium, to a discrete problem that we may write, at a given instant in time, as  $K*T=F$ , where, instead of one differential equation, we have for each time step a set of  $N$  algebraic equations involving the unknown temperatures at  $N$  points in the system (to our choice), a set of known applied stimuli at  $N$  points (to be computed in a particular way), and a set of  $N*N$  coefficients to be computed also in a particular way, depending on the numerical method. Numerical methods differ in the way they yield this system of algebraic equations, but a general baseline exists. The problem may be generally stated as:

$$PDE(T(\vec{x},t))=0, \quad BC(T(\vec{x}_0,t))=0, \quad IC(T(\vec{x},t_0))=0 \quad (72)$$

where  $PDE$ ,  $BC$  and  $IC$  represent functionals related to the partial differential equation, boundary conditions and initial conditions, respectively. Numerical methods approximate the infinite-degrees-of-freedom continuous solution by a finite  $N$ -degrees-of-freedom solution of the form:

$$T^{approx}(\vec{x},t) = T^{IBC}(\vec{x},t) + \sum_{i=1}^N T_i(t)\phi_i(\vec{x}) \quad (73)$$

where  $T^{IBC}(\vec{x},t)$  is a known function (chosen by the modeller) satisfying all the initial and boundary conditions,  $T_i(t)$  are unknown coefficients (varying with time for transient problems) to be numerically found, and  $\phi_i(\vec{x})$  are known trial functions, the base functions the modeller chooses as a function space of the solution. Notice the separation of variables in time and space in (73); in practice, the time-dependence is also discretized, but this is a simpler problem because time is one-dimensional and unidirectional, and we forget it for the moment. Notice also that, in spite of the fact that physical uncertainty comes from different idealisations (geometrical, material, temporal, interactions...), it is customary to look for solutions that approximate the PDE but exactly verifying the initial and boundary conditions.

Several numerical methods have been developed, each with its own advantages and complexities, from simple ones like the lumped method or the finite difference method, which can be developed from scratch for every new problem (but becoming too cumbersome in complex cases), to the standard finite element

method that, once developed (it demands much more effort), can be routinely applied to whatever complex case we have at hand.

Steady state problems in heat transfer are boundary-value problems (elliptic problems), more difficult to solve numerically than initial-value problems (parabolic problems), thus, even for steady state problems, it is advisable to solve the initial value transient until sufficiently-small changes indicate the steady state is reached.

The most common numerical methods, from simpler to more complex, may be grouped as:

- Integral methods, where the integral energy equation  $dE/dt = \dot{Q} + \dot{W}$  is solved, instead of the (differential) heat equation (3). Among them, the most used are:
  - Global fitting, where an ad-hoc continuous  $T$ -field function is fitted.
  - Lumped network, where the system is partitioned in a number of isothermal lumps (a discrete step-wise  $T$ -field).
- Differential methods, where the heat equation is solved (sometimes by integration, but the PDE is apparent), instead of the integral energy equation. Among them, the most used are:
  - Residual minimization.
  - Finite differences.
  - Finite elements.
  - Boundary elements.

Another classification may be in terms of the continuity of the base functions as: global methods (global fitting and residual minimization), and local methods (or partition methods; all the others). The great advantage of local methods is that the base functions can be very simple (often linear). The first step in all local methods is a spatial discretisation of the domain, followed by node assignment (one central or boundary node in the finite difference method, several nodes in the finite element method, at least one at each end), and the choice of base functions, to be explained below.

There are other integral methods, like the Rayleigh-Ritz method, which are based on a variational formulation of the problem if it exists (e.g. minimising the potential energy in mechanical problems or minimising the generation of entropy in thermal problems). The variational functional contains all the information (PDE plus boundary conditions), e.g.  $E = \int f(x, y, y') dx = \min$ , and the unknown coefficients in the temperature fitting are found by directly minimization of the variational, instead of through the equivalent Lagrange equation,  $\partial f / \partial y - d(\partial f / \partial y') / dx = 0$ .

## Global fitting

In the global fitting method, we try to solve the global energy balance equation  $dE/dt = \dot{Q} + \dot{W}$ , instead of the local energy balance that yielded the heat equation (3); i.e. we try to fit the  $T$ -field with a suitable multi-parametric function defined in the whole domain, e.g.,  $T(x, y) = \Sigma(\Sigma(a_{ij}x^i y^j))$ , and the fitting coefficients (in this case the polynomial coefficients) are found by forcing just the global energy balance and some particular boundary conditions of the problem (it is better if the base function already satisfies

the boundary conditions). Unless one succeeds in choosing a 'good' global function, the approximation is usually poor and one has to divide the domain in small elements to be able to use simple fitting functions. A good start is by choosing the most simple function that can accommodate the known boundary conditions. In a sense, global fitting is a kind of integral method, since the global energy balance is obtained by integration of the heat equation to the whole domain (the heat equation was derived inversely).

For our sphere-cooling problem the integral method gets complicated because a simple  $T$ -field cannot be found that is good for short times (when the cooling wave travels from the surface to the centre of the sphere), and for larger times (when the whole sphere is cooling down). We are going to apply the integral method to the very short times of cooling penetration, namely, those for which the one-dimensional planar semi-infinite model applies.

For the planar semi-infinite problem of a step change in surface temperature of a constant-property solid initially at  $T_\infty$  and suddenly brought to  $T_0$ , we want to fit the  $T$ -field by  $T(x,t)=c_0+c_1(x/X)+c_2(x/X)^2+c_3(x/X)^3$ , with the  $c_i$ -coefficients being time-dependent, and  $X$  being the penetration of the thermal change relative to the initial state. Instead of the PDE (solved in [Example 8 in Heat and Mass Transfer](#)), we only make use here of the boundary conditions,  $T(0,t>0)=T_0$ ,  $\partial^2 T(x,t)/\partial x^2|_{x=0}=0$ ,  $T(X,t>0)=T_\infty$ ,  $\partial T(x,t)/\partial x|_{x=X}=0$ , to get the coefficients in terms of the penetration depth  $X$ , and of the energy balance,  $\partial[\int \rho A dx c T(x,t)]/\partial t = -k A d \partial T(x,t)/\partial x|_{x=0}$ , to get the time-evolution of the penetration depth, once the fitted approximation,  $T(x,t)=T_\infty+(T_0-T_\infty)(1-(3/2)(x/X)+(1/2)(x/X)^3)$ , is substituted in the global energy balance; namely,  $X(t)=\sqrt{8at}$ , what can be compared with the exact solution obtained in [Example 8 in Heat and Mass Transfer](#).

For our rod-heated-at-one-end problem, if we assume that the  $T$ -field at steady state can be approximated just by a constant,  $T(x)=c_0$ , imposing the main constrain in the problem, the global energy balance,  $\dot{Q}_{in} = \dot{Q}_{out} \rightarrow \dot{Q}_0 = hpL(T - T_\infty)$ , one gets the solution:  $T = T_\infty + \dot{Q}_0 / (hpL) = 288 + 10 / (20 \cdot \pi \cdot 10^{-2} \cdot 10^{-1}) = 447$  K (to be compared with the analytical result later). If we assume that the  $T$ -field at steady state can be approximated by  $T(x)=c_0+c_1x$ , imposing the main constrain in the problem, the global energy balance,  $\dot{Q}_{in} = \dot{Q}_{out} \rightarrow \dot{Q}_0 = \int_0^L hp(T(x) - T_\infty) dx$ , and an additional one, the local condition at  $x=0$ ,  $\dot{Q}_0 = -kA \partial T / \partial x|_{x=0} = -kAc_1$ , one gets the solution:  $T(x)=(478-636x)$  K (with  $x$  in metres; to be compared with the analytical result later). If we assume that the  $T$ -field at steady state can be approximated by  $T(x)=c_0+c_1x+c_2x^2$ , imposing the main constrain in the problem, the global energy balance,  $\dot{Q}_{in} = \dot{Q}_{out} \rightarrow \dot{Q}_0 = \int_0^L hp(T(x) - T_\infty) dx$ , and two additional ones, the local condition at  $x=0$ ,  $\dot{Q}_0 = -kA \partial T / \partial x|_{x=0} = -kA(c_1 + 2c_2x)_{x=0} = -kAc_1$ , and the local condition at  $x=L$ ,  $-kA \partial T / \partial x|_{x=L} = 0$ , one gets the solution:  $T(x)=(468-636x+3183x^2)$  K (with  $x$  in metres). The above three numerical approximations are shown in Fig. 9 compared with the exact analytical solution, presented in Table 4 (Case 3). As said before, there is little benefit in going to higher-order polynomials, and it might be counterproductive, indeed.

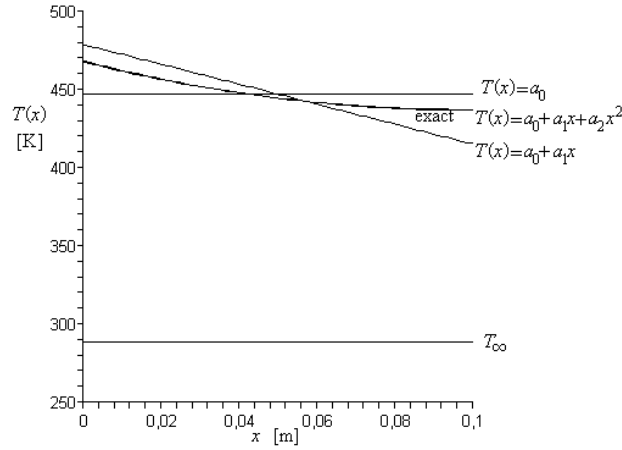


Fig. 9. Comparison of three progressive numerical approximations with the exact solution for the rod-heated-at-one-end problem, at the steady state.

One-dimensional steady-state problems of heat transfer give just ordinary differential equations with boundary values. In this case, besides all numerical methods being studied here, the old shooting method may be applied, what is the transformation of a boundary-value problem into an initial-value problem: the ordinary differential equations are integrated with assumed initial conditions to find end-conditions that at first do not verify the data, but give a residue that can be cancelled by iterations in a root-finder approach. The shooting method may be thought also as a local approximation where the coefficients  $u_i$  are sequentially found by an Euler or Runge-Kutta forward extrapolation.

Of course, the global ad hoc fitting can be extended to include several dimensions and transient effects. For instance, one may try  $T(x,r,t)=T_\infty+(a_0+a_1x+a_2x^2)\cdot(b_0+b_1r+b_2r^2)\cdot(1-\exp(-ct))$  for our rod-heated-at-one-end problem, to find, on top of the axial  $T$ -profile, a radial  $T$ -profile and their time variation from initial rest with the heater off, to the steady state after the heater is set on, with the result:  $T(x,r,t)=288+(180-636x+3183x^2)\cdot(1-109r^2)\cdot(1-\exp(-0.0033t))$ , where  $b_0$  is chosen equal to unity from redundancy in the coefficients,  $b_1$  is equal to zero to preserve axial symmetry,  $b_2$  is computed from the radial energy balance,  $\dot{Q}_0 = \int_0^L -kp \partial T / \partial r|_{r=D/2} dx$ , and  $c$  is computed from the initial energy balance when the heater is switched on,  $\dot{Q}_0 = \int_0^L \rho Ac \partial T / \partial t|_{t=0,r=0} dr$ . Notice however, how clever the choice of the time function has been, already incorporating an exponential temperature increase from rest to steady state.

Finally notice that any numerical method involving only linear equations can be solved explicitly in the parameter variables, and not only numerically, but this advantage is of little help with cumbersome expressions. For instance, the latter solution in algebraic form is:

$$T(x,r,t) = T_\infty + \frac{\dot{Q}_0 L}{kA} f_1(x) f_2(r) f_3(t), \text{ with } f_3(t) = 1 - \exp(-4BiFo), \quad Bi = \frac{hD}{k}, \quad Fo = \frac{kt}{\rho c D^2}$$

$$f_2(r) = 1 - \frac{Bi}{4+Bi} \left( \frac{r}{D/2} \right)^2, \text{ and}$$

$$f_1(x) = \left( \frac{1}{2} + \frac{Bi}{8} \right) \left( \frac{x}{L} \right)^2 - \left( 1 + \frac{Bi}{4} \right) \left( \frac{x}{L} \right) + \left( \frac{1}{3} + \frac{Bi}{12} \right) + \left( \frac{D}{L} \right)^2 \left( \frac{1}{4Bi} + \frac{1}{16} \right) \quad (74)$$

## Lumped network

In the lumped-network method (LNM), a partition of the domain is made in a few elements, manually defined and each of them assumed having uniform temperature, the interactions amongst them manually computed, and the set of coupling algebraic equations automatically solved. It is only used for well-conducting sets of pieces (nearly isothermal in practice), allowing highly nonlinear effects (e.g. radiation coupling).

For our rod-heated-at-one-end problem, if we assume that the  $T$ -field is approximated by three isothermal lumps at  $T_0$ ,  $T_1$ , and  $T_2$ , each comprising a third of the rod, these values can be computed by imposing the energy balances and conductive couplings among them:

$$\begin{aligned}
 \rho c A \frac{L}{3} \frac{dT_0}{dt} &= \dot{Q}_0 - hp \frac{L}{3} (T_0 - T_\infty) - \dot{Q}_1 \\
 \rho c A \frac{L}{3} \frac{dT_1}{dt} &= \dot{Q}_1 - hp \frac{L}{3} (T_1 - T_\infty) - \dot{Q}_2 \\
 \rho c A \frac{L}{3} \frac{dT_2}{dt} &= \dot{Q}_2 - hp \frac{L}{3} (T_2 - T_\infty) - 0 \\
 \text{with } \dot{Q}_1 &= kA \frac{T_0 - T_1}{L/3} \quad \& \quad \dot{Q}_2 = kA \frac{T_1 - T_2}{L/3}
 \end{aligned} \tag{75}$$

At steady state, we can solve the system of five equations with five unknowns, with the solution:  $T_0=460$  K,  $T_1=447$  K,  $T_2=433$  K,  $\dot{Q}_1=6.4$  W (the heat flux passing from the first to the second lump), and  $\dot{Q}_2=3.1$  W (the heat flux passing from the second to the third lump). A comparison of this numerical solution with the exact solution is shown in Fig. 10. Notice that, as before, analytical expressions can be obtained for the lumped parameters in linear systems.

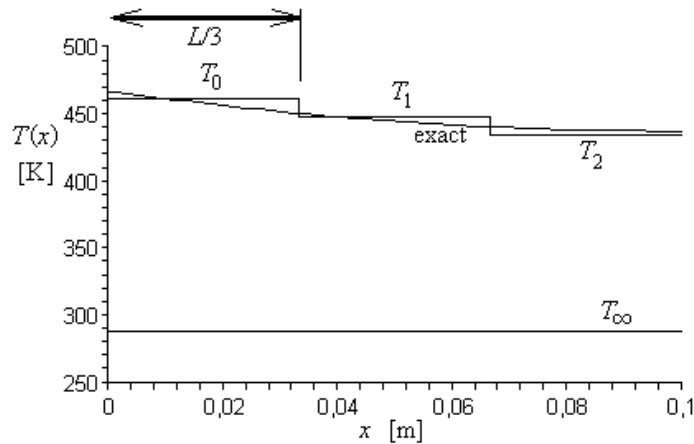


Fig. 10. Comparison of a three-lump numerical approximation with the exact solution for the rod-heated-at-one-end problem.

Related to the lumped network is the more structured finite volume method (FVM), where a partition of the domain is made in a regular mesh, e.g. a square mesh of size  $h$  in 2D, and the integro-differential equation of energy balance, e.g.  $\rho c V dT_i/dt = \sum Q_{Ai}$ , is applied to each element, which is considered to have uniform temperature  $T_i$ . The heat exchanges with the neighbours are averaged with a mean thermal conductivity and mean thermal gradient. For simple averaging, the FVM usually yield the same nodal

equations as the FDM, the difference been in the strictly mathematical approach in FDM and the more physical one in FVM.

## Spectral methods

Most numerical methods asymptotically approach the continuous solution by a spatial discretization of the function, but spectral methods do it by a discrete series of continuous functions with appropriate coefficients (the set of coefficients is seen as the 'spectrum' of the solution), as set in (73). The main advantage of using continuous base functions is the easiness of derivation (recall we are dealing with complicated PDE).

Spectral methods try to approximate the function (solution) by increasing the number of modes or parameters in a given space of functions, e.g. approximating  $T(x)=\sum a_i x^i$  and increasing the number of terms  $i$ , or better using orthogonal functions like  $T(x)=\sum a_i \sin(i\pi x)$ , etc. Although any function can be approximated by an infinite series expansion of any kind, if the base functions are orthogonal the coefficients in the series are uncoupled and a lot of work is saved (they can be found independently, and if their number is increased, only the added ones must be computed).

Spectral methods usually take the domain globally (i.e. one element with multi-parametric base function), but some new methods take a local approach, in combination with spatial methods. The handicap of spectral methods is that for a multi-parametric fit of a global base function, unless one succeeds in choosing a 'good' global function, the approximation is usually poor and misleading (e.g. with ripples), and it is better to divide the domain in small elements to be able to use simple fitting functions (spatial methods), e.g. piece-wise linear polynomials for second order PDE.

## Residual fitting

As in the global fitting method, we try to fit the  $T$ -field with a suitable multi-parametric function defined in the whole domain,  $T(\vec{x},t) = \sum c_i(t)\phi_i(\vec{x})$ , but the coefficients now are determined by minimization of the residuals obtained when the fitting function is substituted into the differential form of the problem:

$$PDE\left(\sum_{i=1}^N c_i(t)\phi_i(\vec{x})\right) = R(\vec{x},t) = \min, \text{ for independent } c_i \quad (76)$$

where the minimization of the  $N$ -degree-of-freedom residual is accomplished by weighted averaging in the spatial domain:

$$\langle w_i(\vec{x}), R(\vec{x},t) \rangle = 0, \quad i = 1..N \quad (77)$$

where  $w_i$  are the weighting functions and  $\langle w_i, R \rangle$  is the projection or scalar product.

For instance, for our rod-heated-at-one-end problem at the steady state, the differential problem was stated as (25):

$$0 = \frac{d^2 T}{dx^2} - \frac{hp}{kA}(T - T_\infty) \quad \text{with} \quad \dot{Q}_0 = -kA \frac{dT}{dx} \Big|_{x=0} \quad \& \quad 0 = -kA \frac{dT}{dx} \Big|_{x=L} \quad (78)$$

If we chose as fitting function  $T(x) = c_0 + c_1 x + c_2 x^2$ , imposing the two boundary conditions we get  $c_2 = \dot{Q}_0 / (2kLA)$  and  $c_1 = -\dot{Q}_0 / (kA)$ , and the other coefficients (only  $c_0$  here) are obtained by proper minimization of the following weighted residual,  $R(c_i)$ :

$$R(c_i) \equiv \int_{x=0}^{x=L} \left( \frac{d^2 \bar{T}(x)}{dx^2} - \frac{hp}{kA} (\bar{T}(x) - T_\infty) \right) w_i(x) dx \quad (79)$$

obtained by integration, over the whole domain (here the length of the rod), of the differential equation that should be zero if exact, multiplied by some appropriate weighting functions,  $w_i(x)$ , which can be chosen following different approaches, to be explained below:

$$\begin{cases} w_i(\bar{x}) = \delta(\bar{x} - \bar{x}_i) & \text{method of collocation, and finite differences (FDM)} \\ w_i(\bar{x}) = \partial R / \partial u_i & \text{method of least squares (LSM)} \\ w_i(\bar{x}) = \phi_i(\bar{x}) & \text{method of finite elements of Galerkin (FEM)} \end{cases} \quad (80)$$

If we substitute our numerical values in (79) yields  $R(c_i) = \int (17890 - 40c_0 + 25460x - 127000x^2) w_i(x) dx$ .

### Collocation method

In this case,  $w_i(x)$  in (79)-(80) are just delta functions at each of a discrete-set of points where we want to cancel the residual  $R(c_i)$ . As we only have one remaining coefficient in our example,  $c_0$ , we impose the cancellation of the residual at, say, the mid-point in the rod,  $x=L/2$ , obtaining  $c_0 = T_\infty + (\dot{Q}_0 L / (kA))(3/8 + 1/(m^2 L^2))$ , which, by substitution of our sample-problem data finally yields  $T(x) = 471 - 636x + 3183x^2$  with  $x$  in metres, to be compared with the exact solution in Fig. 11 below.

### Least square method (LSM)

In this case,  $w_i(x)$  in (79)-(80) coincides with the PDE residual, i.e. the sought coefficients are found by minimization of the integration of the squares (least square method):  $R(c_i) = \int (17890 - 40c_0 + 25460x - 127000x^2)^2 dx = \min$ . As we only have one remaining coefficient,  $c_0$ , we impose  $\partial R(c_i) / \partial c_0 = 0$ , obtaining  $c_0 = T_\infty + (\dot{Q}_0 L / (kA))(1/3 + 1/(m^2 L^2))$ , which, by substitution of our sample-problem data finally yields  $T(x) = 468 - 636x + 3183x^2$  with  $x$  in metres, to be compared with the exact solution in Fig. 11 below.

### Galerkin method

In this case,  $w_i(x)$  in (79)-(80) are each of the base functions of the unknown terms used for the  $T$ -field, i.e.  $w_i(x) \equiv \phi_i(x)$  with  $T(\bar{x}, t) = \sum c_i(t) \phi_i(\bar{x})$ . Here we have used as  $\phi_i(x)$  the monomials 1,  $x$  and  $x^2$ , but only the independent term  $c_0$  was left unknown, thus, for the Galerkin method we must solve  $R(c_i) = \int (17890 - 40c_0 + 25460x - 127000x^2) dx = 0$ . It happens for this example that this solution coincides with the least square solution. Figure 11 shows the different approximations using the residual fitting approach, in comparison with the exact analytical solution.

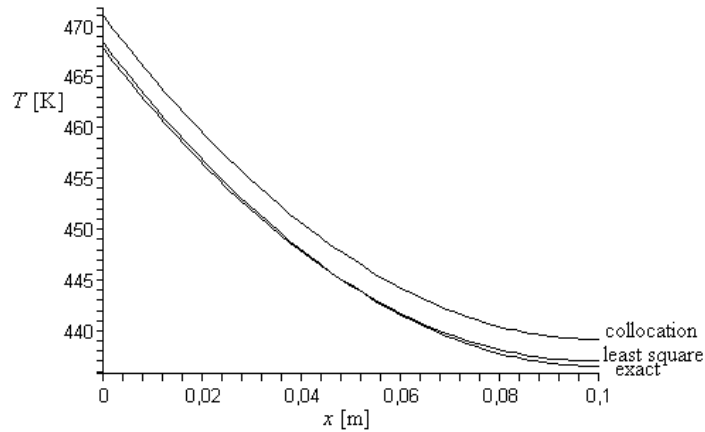


Fig. 11. Comparison of two numerical approximations (collocation and least square) using  $T(x)=c_0+c_1x+c_2x^2$ , with the exact solution for the rod-heated-at-one-end problem at the steady state (Case 3 in Table 4).

## Finite differences

In the finite difference method (FDM), invented by Courant et al. in 1929, the partial differential equation is discretized term by term, substituting each derivative by its truncated Taylor expansion. The minimum order for time derivatives is a linear approach, usually advanced in time, namely  $\partial T/\partial t \approx (T(t+\Delta t) - T(t))/\Delta t$ , whereas for spatial derivatives at least a second order development is needed to approach second-order derivatives,  $\partial^2 T/\partial x^2 \approx (T(x+\Delta x) - 2T(x) + T(x-\Delta x))/(\Delta x)^2$ ; first order derivatives are usually approximated by a central difference,  $\partial T/\partial x \approx (T(x+\Delta x) - T(x-\Delta x))/(2\Delta x)$ , to avoid bias when choosing forward or backward differences. Notice that, although the central difference is a better approximation (2nd order) than either the forward or backward differences (1st order), using it for time would complicate too much the computation. Higher-order discretisation of the derivatives provide a more precise fitting of the function, at the expense of more complication (but the overall computing resources may be reduced if a coarser grid is good enough).

The FDM can be also viewed as a discretized mesh with the PDE integrated at each finite volume. To each finite volume, a nodal point is assigned, to which the unknown temperature is attributed, as in the lumped network approach. The FDM yields a highly structured system of equations, particularly when a regular mesh is used, what has its pros and cons: the main advantage is the simple formulation of the method, what renders it the basic numerical method to solve PDEs; the penalty is that FDM demands a simple geometry with a structured grid, i.e. FDM becomes complicated in systems with non-rectangular (or non-cylindrical, or non-spherical) geometries.

FDM starts by establishing a mesh of nodes in the domain, i.e. a set of points in space where the function is to be computed. There should be a node where the function is sought; at least one node at each boundary or singularity, plus a few others for better resolution. Although not mandatory, it is most advisable to use a regular mesh to simplify the coding. To each node, a material element is ascribed; to each node a thermal inertia is assigned, and to each pair of nodes a thermal conductance is assigned. The finite difference discretization of the PDE provides the energy balance to every generic (internal) node; the energy balance must be set aside for each special (interface) node, which are really the most characteristic data in a problem. It is advisable to include one artificial node at each extreme to represent



the boundary conditions at infinity. A regular spatial mesh is used, e.g. a square mesh of size  $h$  in 2D, and derivatives approximated by finite differences, centred in the node, or from one side (forward or backward). For instance, the Laplace operator is approximated at every standard internal node (marked by its  $x$ -step position  $i$  and its  $y$ -step position  $j$ ), using centred differences, by:

$$\nabla^2 T_{i,j} \approx \frac{1}{h^2} (T_{i-1,j} + T_{i+1,j} + T_{i,j-1} + T_{i,j+1} - 4T_{i,j}) \quad (81)$$

a simple discretization that becomes cumbersome when applied to boundary nodes if the geometry is not rectangular; e.g., for boundary nodes that have only a fraction  $f$  of an  $h$ -step in the North-South-East-West neighbour, the Laplace operator should be approximated by:

$$\nabla^2 T_{i,j} \approx \frac{2}{h^2} \left( \frac{1/f_W}{f_W + f_E} T_{i-1,j} + \frac{1/f_E}{f_W + f_E} T_{i+1,j} + \frac{1/f_S}{f_S + f_N} T_{i,j-1} + \frac{1/f_N}{f_S + f_N} T_{i,j+1} - \frac{f_S f_N + f_W f_E}{f_S f_N f_W f} 4T_{i,j} \right) \quad (82)$$

and becomes even more awkward because, for a regular mesh in an irregular domain, a mesh refinement doesn't include all previous nodes in the boundary).

For a steady problem with  $N$  nodes, the set of  $N$  algebraic equations with  $N$   $T$ -unknowns can be solved directly by matrix inversion, or indirectly by an iterative method, for instance using  $T_{i,j,\text{new}} = (T_{i-1,j} + T_{i+1,j} + T_{i,j-1} + T_{i,j+1})/4$  to solve for Laplace equation,  $\nabla^2 T = 0$ . An iterative relaxation method in which  $T_{i,j,\text{better}} = T_{i,j,\text{new}} + W(T_{i,j,\text{new}} - T_{i,j,\text{old}})$ , with a weighting factor  $0 < W < 1$ , is usually the best.

For transient problems, the computation of temperature at the nodes at time  $t + \Delta t$  can be based on  $T$ -values at time  $t$  (the explicit method, the most used, although it may become unstable), can be based on  $T$ -values at time  $t + \Delta t$  (the implicit method, always stable but requiring the inversion of a matrix), or in a wise combination of the two, named the Crank-Nicholson method. A general stability criterion for the explicit method is that every central coefficient (what multiplies  $T_{i,j}$  at previous time  $t$ ) be non-negative ( $\geq 0$ ); in a one-dimensional case with convective ends, that coefficient is  $(1 - 2Fo(1 + Bi))$ , with  $Fo = a\Delta t / \Delta x^2$  and  $Bi = h\Delta x / k$ , and thus  $Fo < 1 / (2(1 + Bi))$ , what means that very small time increments and a lot of time steps are required (doubling the number of nodes, multiplies by four the computation time).

The stability criterion can be explained in terms of the Second Law of Thermodynamics if we imagine the thermal relaxation of a node at  $T_1$  with the surroundings nodes at  $T_0 < T_1$  (2 in one-dimensional problems); the discretized heat equation can be written as  $\Delta_t T / \Delta t = 2a\Delta_x T / (\Delta x)^2$ , but the Second Law forbids the temporal variation  $\Delta_t T$  to surpass the spatial variation  $\Delta_x T$ , i.e.  $\Delta_t T < \Delta_x T$ , implying  $2a\Delta t / (\Delta x)^2 < 1$  or  $Fo < 1/2$ .

For our rod-heated-at-one-end problem, we pass from the partial differential formulation of the problem:

$$\frac{\partial^2 T}{\partial x^2} - \frac{hp}{kA} (T - T_\infty) - \frac{1}{a} \frac{\partial T}{\partial t} = 0, \quad \text{with } \dot{Q}_0 = -kA \frac{\partial T}{\partial x} \Big|_{x=0}, \quad 0 = -kA \frac{\partial T}{\partial x} \Big|_{x=L}, \quad T \Big|_{t=0} = T_\infty \quad (83)$$

to the finite difference formulation, or nodal equations, either built as an energy balance of the finite volumes:

$$\rho A \Delta x c \frac{T_i^{j+1} - T_i^j}{\Delta t} = k A \frac{T_{i+1}^j - T_i^j}{\Delta x} - k A \frac{T_i^j - T_{i-1}^j}{\Delta x} - h p \Delta x (T_i^j - T_\infty)$$

with  $\dot{Q}_0 = -k A \frac{T_1^j - T_0^j}{\Delta x}$ ,  $0 = -k A \frac{T_N^j - T_{N-1}^j}{\Delta x}$ ,  $T_i^0 = T_\infty$  (84)

or directly by Taylor expansion of the PDE formulation:

$$\frac{T_{i+1}^j - 2T_i^j + T_{i-1}^j}{(\Delta x)^2} - \frac{h p}{k A} (T - T_\infty) - \frac{1}{a} \frac{T_i^{j+1} - T_i^j}{\Delta t} = 0$$

with  $\dot{Q}_0 = -k A \frac{T_1^j - T_0^j}{\Delta x}$ ,  $0 = -k A \frac{T_N^j - T_{N-1}^j}{\Delta x}$ ,  $T_i^0 = T_\infty$  (85)

by establishing the mesh of nodes with the guidelines given above (superscript  $j$  is for time steps and subscript  $i$  for spatial steps), as shown by the large dots in Fig. 12.

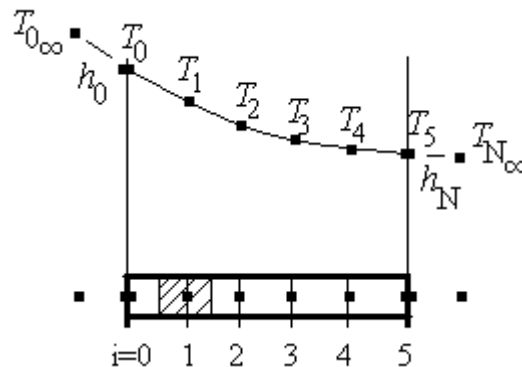


Fig. 12. Finite difference discretization for the rod-heated-at-one-end problem.

From the initial  $T$ -field,  $T(x,0)$ , the new  $T$ -values at time  $t+\Delta t$  can be explicitly stated in terms of the older  $T$ -values, or implicitly stated in terms of the present  $T$ -value; in any case, special care for the boundary nodes is required. Introducing  $Fo \equiv a \Delta t / (\Delta x)^2$  and  $\beta \equiv 2Fo(1 + (2hR/k)(\Delta x/R)^2)$ , the explicit formulation in our example (Fig. 12) is:

$$\begin{bmatrix} T_0^{j+1} \\ T_1^{j+1} \\ T_2^{j+1} \\ T_3^{j+1} \\ T_4^{j+1} \\ T_5^{j+1} \end{bmatrix} = \begin{bmatrix} 1-\beta & 2Fo & 0 & 0 & 0 & 0 \\ Fo & 1-\beta & Fo & 0 & 0 & 0 \\ 0 & Fo & 1-\beta & Fo & 0 & 0 \\ 0 & 0 & Fo & 1-\beta & Fo & 0 \\ 0 & 0 & 0 & Fo & 1-\beta & Fo \\ 0 & 0 & 0 & 0 & 2Fo & 1-\beta \end{bmatrix} \times \begin{bmatrix} T_0^j \\ T_1^j \\ T_2^j \\ T_3^j \\ T_4^j \\ T_5^j \end{bmatrix} + \begin{bmatrix} \frac{2\dot{Q}_0\Delta t}{\rho c A \Delta x} + \frac{ph\Delta t}{\rho c A} T_\infty \\ \frac{ph\Delta t}{\rho c A} T_\infty \\ \frac{ph\Delta t}{\rho c A} T_\infty \\ \frac{ph\Delta t}{\rho c A} T_\infty \\ \frac{ph\Delta t}{\rho c A} T_\infty \\ \frac{ph\Delta t}{\rho c A} T_\infty \end{bmatrix} \quad (86)$$

whereas the implicit formulation is:

$$\begin{bmatrix} -1-\beta & 2Fo & 0 & 0 & 0 & 0 \\ Fo & -1-\beta & Fo & 0 & 0 & 0 \\ 0 & Fo & -1-\beta & Fo & 0 & 0 \\ 0 & 0 & Fo & -1-\beta & Fo & 0 \\ 0 & 0 & 0 & Fo & -1-\beta & Fo \\ 0 & 0 & 0 & 0 & 2Fo & -1-\beta \end{bmatrix} \times \begin{bmatrix} T_0^{j+1} \\ T_1^{j+1} \\ T_2^{j+1} \\ T_3^{j+1} \\ T_4^{j+1} \\ T_5^{j+1} \end{bmatrix} = \begin{bmatrix} T_0^j + \frac{2\dot{Q}_0\Delta t}{\rho c A \Delta x} + \frac{ph\Delta t}{\rho c A} T_\infty \\ T_1^j + \frac{ph\Delta t}{\rho c A} T_\infty \\ T_2^j + \frac{ph\Delta t}{\rho c A} T_\infty \\ T_3^j + \frac{ph\Delta t}{\rho c A} T_\infty \\ T_4^j + \frac{ph\Delta t}{\rho c A} T_\infty \\ T_5^j + \frac{ph\Delta t}{\rho c A} T_\infty \end{bmatrix} \quad (87)$$

where factor 2 in the boundary equations (first and last rows in the matrices) come from those nodes being chosen to have half the mass of the other (see Fig. 12). The implicit formulation requires the inversion of a big matrix, although in our case (and in many other) it is a tri-diagonal matrix quickly inverted, the explicit formulation not requiring such an inversion, but demanding a very small time step to avoid instability in the iteration, guarantying at least  $Fo \equiv a\Delta t / (\Delta x)^2 < 1/2$ , what, with our rod-heated-at-one-end problem data and having chosen  $\Delta x = L/5 = 0.02$  m, means that  $\Delta t < (\Delta x)^2 / (2a) = 2.4$  s, demanding a lot of iterations to reach the steady state (formerly evaluated in [Exercise 3 in Heat and Mass Transfer](#) to be some 1200 s). A better approximation, using  $N=20$  instead of  $N=5$ , and 10 000 time steps, is presented in Fig. 13.

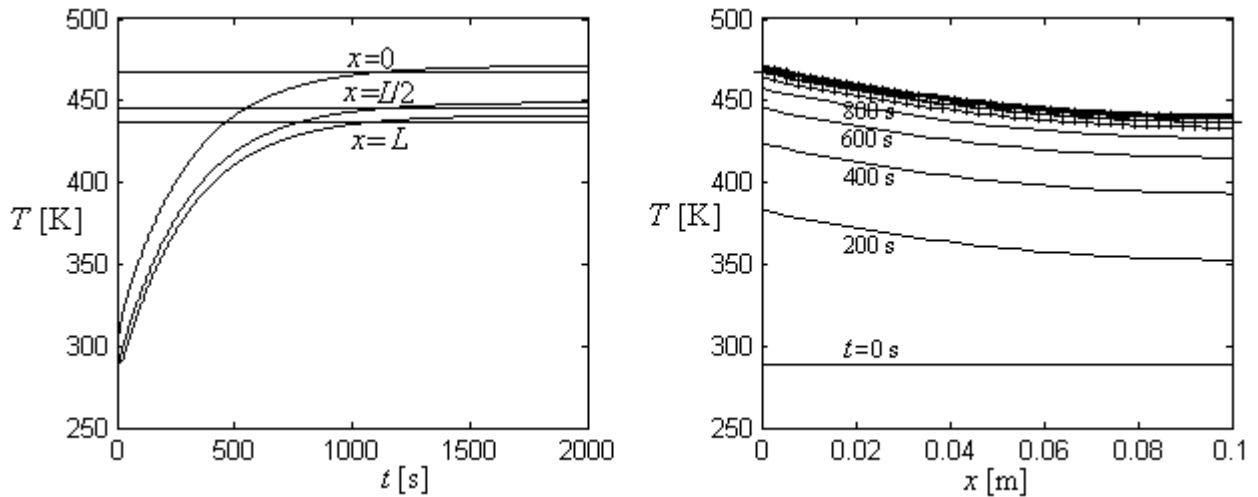


Fig. 13. Comparison of a finite difference numerical approximation with the exact solution for the rod-heated-at-one-end problem.

[Example 3. Satellite platform with embedded battery modules.](#)

[Example 4. Thermal transients in a CFRP wall.](#)

[Example 5. Printed circuit board with central dissipation.](#)

[Example 6. Printed circuit board with two large integrated circuits](#)

[Example 7. Kapton heater between plates](#)

## Finite elements

The finite elements method (FEM, also known as finite element analysis, FEA), invented by Courant in 1943, is based on the Galerkin procedure to minimise residuals, seen above. In the simplest FEM formulation, the spatial domain is discretized in triangles (for 2D domains), and the base functions are chosen as linear unitary local functions (i.e. zero outside their associated element). Notice that the subsystem in FEM is a mass between nodal points at the corners, whereas the subsystem in FDM is a mass around the nodal point.

Standard algorithms exist to mesh any irregular domain, and because here the approximation is by integration (that with suitable base functions may be done locally in each element without any directionality) instead of by differentiation (that is a directional operation based on all neighbour elements), the procedure to do it automatically is well developed. The task is massive but simple (ideal for computers), thus finite element is the preferred numerical method for (non-singular) engineering problems, particularly for multidisciplinary computations (mechanical, thermal, fluid-dynamic, electrical). Typical commercial FEM-packages are: ABAQUS, ANSYS, FEMLAB, FLUENT, MSC/NASTRAN... These packages usually cover a wide spectrum of possibilities (e.g. materials properties and heat sources varying with time), and they solve very general PDE like:

$$a_1 \frac{\partial T}{\partial t} + a_2 \frac{\partial^2 T}{\partial t^2} + \sum_{i=1}^3 \frac{\partial}{\partial x_i} \left( b_{1,i}(x_i) \frac{\partial T}{\partial x_i} \right) + \sum_{i=1}^3 \frac{\partial}{\partial x_i} \left( b_{2,i}(x_i) \frac{\partial^2 T}{\partial x_i^2} \right) + c(x_1, x_2, x_3) T = f(t, x_1, x_2, x_3) \quad (88)$$

[Example 8. Insulated box with internal heating](#)

## **Boundary elements**

Because a given set of boundary and initial conditions uniquely define the solution in the domain, the value of the function at any point in the interior can be expressed as a sole contribution of boundary values, what is achieved mathematically by the Green-Stokes-Gauss-divergence theorem, which is the foundation of the boundary elements method (BEM). With this method, first the full solution (function and derivatives) at the boundary points are computed by a kind of finite-element method where the base functions are the fundamental solutions of the PDE at the boundary nodes, then solving a set of algebraic equations at the nodes, and finally, if needed, the value at any internal point is directly computed by a quadrature (without interpolation). The problem with the boundary element method is that the local integration in the boundary are more involved than in the standard FEM because there are singular points that require more elaborated computations. Other handicap is that the BEM only applies to regions of constant properties. The great advantage is that for bulky domains the number of nodes significantly decreases, particularly for infinite domains (what explains its massive use in external fluidmechanics and geomechanics). Incidentally, for infinite domains, besides the BEM, one may also resort to classical FEM with a truncated domain progressively enlarged, or matched to an asymptotic analytical expansion, or stretching the external elements with a log-transformation.

[Back to Heat and mass transfer](#)

[Back to Thermodynamics](#)